Electric design of the Power Processing Unit for Pulsed Plasma Thrusters for CubeSat applications.

Marco A. Sanromán Reséndiz

School of Electrical Engineering

Thesis submitted for examination for the degree of Master of Science in Technology.

Espoo, Finland / Tainan, Taiwan

Thesis supervisor:

Prof. Jaan Praks

Thesis advisor:

PhD. Jordan Vannitsen

space master

Aalto University
School of Electrical
Engineering

LULEÅ
UNIVERSITY
OF TECHNOLOGY

AALTO UNIVERSITY
SCHOOL OF ELECTRICAL ENGINEERING

ABSTRACT OF THE
MASTER'S THESIS

Author: Marco A. Sanromán Reséndiz

Title: Electric design of the Power Processing Unit for Pulsed Plasma Thrusters for CubeSat applications.

Date: Language: English Number of pages: 6+72

Department of Radio Science and Technology

Professorship: Space Robotics

Supervisor: Prof. Jaan Praks

Advisor: PhD. Jordan Vannitsen

The opening of space to the private and academic sector has cause a rapid increase in the activities on this field during the last two decades. This movement is known as *New Space*, where by creating collaborations between governments, private industry and universities is defining what could be the new space race. The use of nano-satellites, in special CubeSats, the creation of more specific missions has risen with them the necessity of more complex subsystems. Odysseus Space Inc in collaboration with the National Cheng Kung University (NCKU), decided to create a propulsion system where Pulsed Plasma Thrusters (PPTs) are targeted as an Attitude Control System (ACS) for CubeSats. Pulsed Plasma Thrusters have a great legacy being the first electric propulsion thruster to flight in space. Nevertheless, PPTs faced an apparent abandonment for the use of more efficient technologies, it has been brought to CubeSats due its robustness and scalability.
This work presents different approaches to develop a modular power processing unit (PPU) for PPTs for Cubesats applications, resulting in a functional PPU which meets the tight budget of 10X10X10 cm that conforms the CubeSat Unit standard. Each chapter covers a brief review of the concepts, their analysis and the description of their development while facing the challenges that brings to manage voltages in the order of kilo volts in such small spatial budget. Finally, using a combination of high gain Fly-back and Cockcroft-Walton voltage multiplier topologies for the sparkplug circuit, a main discharge and control circuit are prototyped and tested as part of the PPU, making the baseline for further investigations.

Keywords: Space technology, CubeSat, nano-satellite, electric propulsion, PPT, PPU

Preface

This work is a sum of efforts between the author and diverse institutions, where an investigation for the miniaturization of the first means of space propulsion was developed, targeting the New Space era by fitting them into the CubeSat satellites.

I would like to thanks the Aalto University, specially to Jaan Praks who had the role as my supervisor, the LuLeå University of Technology for giving me the opportunity to be part of these huge family that the SpaceMaster is. Also I have to mention the great hospitality I received from the Odysseus Space Team in Taiwan, in special thanks to Jordan Vannitsen for the trust he gave me and the chance to go and work into this fascinating field in the other side of the globe.

In the same way I want to have a mention to all my classmates from the Space-Master Round 13, for all those unforgettable moments we had together, from the cultural dinners and crazy parties to the stressful moments of hard work. Without any doubt these last 2 years wouldn't have been the amazing experience of what it was.

Thanks to the Fusion Research Group(GIF), who encouraged me to embark towards the unknown in search of the truth. To the national council of science and technology -CONACYT- in Mexico, for have granted me with the scholarship to course this degree.

Finally but not least, my loved family who from the other side of the world where always present at every step I made until here. You are my all!

Thank you!
Gracias!

Otaniemi, 31.12.2019

Marco A. Sanroman R. Engineer

"For forty years I have worked on the reactive engine and have felt that the journey to Mars would not begin for many hundreds of years. But times are changing. I believe that many of you will be witnesses to the first voyage beyond the atmosphere."
K.E. Tsiolkovsky. 1 May 1933.

Contents

Abbreviations

AC	Alternating Current
ACS	Attitude Control System
ACDS	Attitude Control and Determination System
CCM	continuous conduction mode
C-WVM	Cockroft-Walton Voltage Multiplier
COTS	Consumer Off-The-Shelf
DC	Direct Current
DCM	Discontinuous Conduction Mode
EP	Electric Propulsion
EPS	Electronic Power System
ESA	European Space Agency
FB	Fly-Back
GEO	Geo-stationary Orbit
J	Joules
kV	Kilo Volts
LEO	Low Earth Orbit
LTU	Lulea Tekniska Universitet
NASA	National Aeronautics and Space Administration
NCKU	National Cheng Kung University
NSPO	National Space Program Office
MDC	Main Discharge Circuit
OBC	On Board Computer
PPT	Pulsed Plasma Thruster
PPU	Power Processing Unit
PTFE	Polytetrafluoroethylene (Teflon)
sec	Seconds
SPC	Spark Plug Circuit
U	CubeSat Unit. 10x10x10 cm
USA	United States
USSR	Union of Soviet Socialist Republics
ZAPLab	Zic and Partners Laboratory

1 Introduction

As most space-related technologies, the major advances recall from the cold war, when the Soviet Union (USSR) and the United States (USA) where competing to establish a military dominance in space, what can be called the first space race. Since then and even after the falling of the USSR becoming what today we know as Russia, the space domain was uniquely controlled by governments. Nevertheless at the beginning of the 2000's, the concept of CubeSat Unit (1U), a satellite with dimensions about 10x10x10 cm and no more than 1.3 kg mass, brought an unexpected revolution in what space field means, marking a new era known as New-Space [3].

Although the effervescence that New-Space has brought, the concepts used during the cold war have been still applied by space engineers during the last 50 years, and as is expected, the use of PPTs is not an exception. PPTs dates back to the Soviet Mars probe Zonda-2 launched in 1964 towards the red planet, where this propulsion system was used for first time. The probe was equipped with 6 PPTs to provide 3 axis attitude stabilization, leaving with it a great amount of literature and making history as the first electrical propulsion in the history of the space flight[1] [5] [9].

Since then, the concept was dropped and partially replaced by more efficient technologies as Ion thrusters, hall-effect, resistojets, cold gas, etc. Nonetheless, the emergence of the New Space has brought an easier access to space to universities and private sector by nano and pico satellites. Consecutively a new market has been opened where the demand for the miniaturized systems that drive these satellites has increased significantly during the past 10 years, bringing with it all the necessities of traditional spacecrafts. Therefore, PPTs have been retaken by the academy and industry, mainly due its relatively simplicity, low number of parts, no necessity of tanks to storage its fuel and compact structure, facilitating in this way its scalability into the CubeSat standard. Some of the latest attempts to bring them back have been carried out by the Surrey space center in UK who in 2013 included a set of 8 micro PPTs in the 3U CubeSat STRaND-1 mission [10]. Mars Space LTD and Clyde Space also in the UK [11], one of the companies leader in nanosatellites solutions, who together have a completely set for orbit station keeping since 2016 while other universities in the USA, Japan, Germany, Italy and Iran have shown increasing interest on this technology.[10][18][17]

Whereas the scheme robustness is one of the main attractive of PPTs, one of the biggest challenges for its inclusion in CubeSats lies in its operational principle of controlling a high voltage discharge within the small space a 1U CubeSat is and the effects this burst has on the performance of the system itself. One of the common issues mentioned in the literature is the carbon coating formation in the igniter as result of the ablation of the PTFE as part its working principle. In addition the power electronics needed is usually difficult to manipulate within nanosatellites due its bulky size and clearance between components working at high tensions is limited by an area of 10 cm^2.

Thereby, this work presents a modular power processor unit (PPU) for an array of 4 thrusters for attitude control. It includes the power stage, where the voltage coming from the Electronics Power System (EPS) is stepped up to 8-10 kV. The high power storage stage on charge to provide a targeted 6 μNs total impulse controlled by a basic control system test bench. Moreover and recalling some of the lessons encounter in the literature, a totally free-mechanical trigger is developed while a galvanic isolation keep independent the power stage to the logic stage.

During the development of this thesis, was spotted the possibility of a customized scalability depending of the necessities of the mission, where not only an attitude control would be possible but orbit keeping could be aimed. In this way was how a modular configuration of the power stages was designed, allowing the easy scaling of the system from 1 up to 8 thrusters.

For the spark plug circuit, a flyback topology was used to initially step up the voltage from 5 volts to 1 kV. Then an array of 8 stages Cockcroft-Walton voltage multiplier was the responsible to deliver the targeted 8 kV to a small capacitor bank located right before the physical sparkplug. Parallel to this, a main discharge circuit was designed to develop a maximum energy of 5 Joules per discharge. For this, the generation of a regulated 2 kV DC was provided using an array of DC-DC converters from the EMCO series, which main characteristic was the possibility of controlling its output voltage, and consequently its power consumption and thrust by software. Finally, either the discharge and the main discharge energy were controlled by a basic control schema using a Atmega328 microcontroller, which by pulse modulation allowed to control the charge and discharge of the system.

Along the 5 months that this work lasted and summing efforts between the ZAP lab of the National Chen Kung University and Odysseus Space, was developed a engineering model formed by 4 thrusters, offering a quality twat bench for future investigations. The project was divided in 4 main stages, where 3 of them are: Spark plug circuit, Main discharge circuit and Control platform. Being the fourth one the mechanical design of the main body and sparkplug, which is not covered by this work.

2 Pulsed Plasma Thrusters

In the following chapter will be described a comprehensive review of the working principle of the PPTs, where are tackled topics as the history, fundamental theory and work schema for the development of the ARGO project. This chapter is aim to introduce the reader with the basic knowledge to follow the subsequently sections of this work.

2.1 Introduction to electric propulsion

An electric propulsion system is such subsystem intended to provide kinetic energy by transforming the electric power supplied by the EPS on board the S/C using a propellantas an agent to provide thrust. Typically this process is managed by a subsection known as the power processing unit or PPU. Therefore, the PPU processes the requirements of the OBC and convert the raw power coming from the EPS into the specific proportion required by each kind of thruster. This task make the PPU usually the one of the most challenging subsystem of the EP.[2]

In Figure 1 is pictured the PPU developed by Airbus for the GOCE mission, which was making use of an Ion thruster.

Additionally to its main function, usually the PPU is on charge of more complex tasks such as:

- Full control of the system; start up, thrust control, shut down.
- Monitoring the subsystems.
- Failure detection and recovery mode.

It can be said, that its main goal is to drive the EP almost autonomously, leaving apart the OBC intervention except for switching on/off the system and data handling.

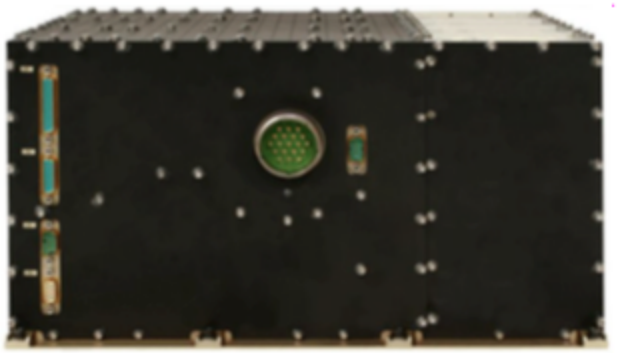

Figure 1: Airbus's PPU for the GOCE ion thruster mission.

After the PPU, the energy has to be induced to the main system and because of it, each type of thruster is defined by how they make use of the available power to produce thrust. As it is always easier to interpret a topic if this is narrowed and classified, within the EP systems it can be done by understanding the working principle of each technology, therefore, they will be boarded in the following classification. See Figure 2.

Electrothermal

Commonly, this kind of thrusters works as a normal motor rocket. Where through a heat source heat up the propellant until this is expanded and then accelerated out using a throat and a nozzle, generating thrust by the second expansion at the output. Depending how the heat is generated, they can be either resistojet or arcjet. [4]

Electromagnetic

These thrusters use the electromagnetic force, known as a Lorentz force,to accelerate ionized plasma in the perpendicular direction to its magnetic field. Thereby, the Lorentz force is who provide the thrust. Within this classification, exist primary the PPTs and the MPDT, which its main difference lies on the way in how each one ionize the propellant. While PPTs use a pulsed plasma discharge, the MPDT uses a continuous high current arc.[4]

Electrostatic

Thrusters whose particles are accelerated by the Coulomb's force, are categorized in this section. The Coulombs force is a function of the static electric field which is perpendicular to a magnetic field. These are perhaps the most efficient type of thruster. Nevertheless, its construction usually involves several processes as micro or nano mechanics. Making them very sensitive to the manufacture accuracy.[4]

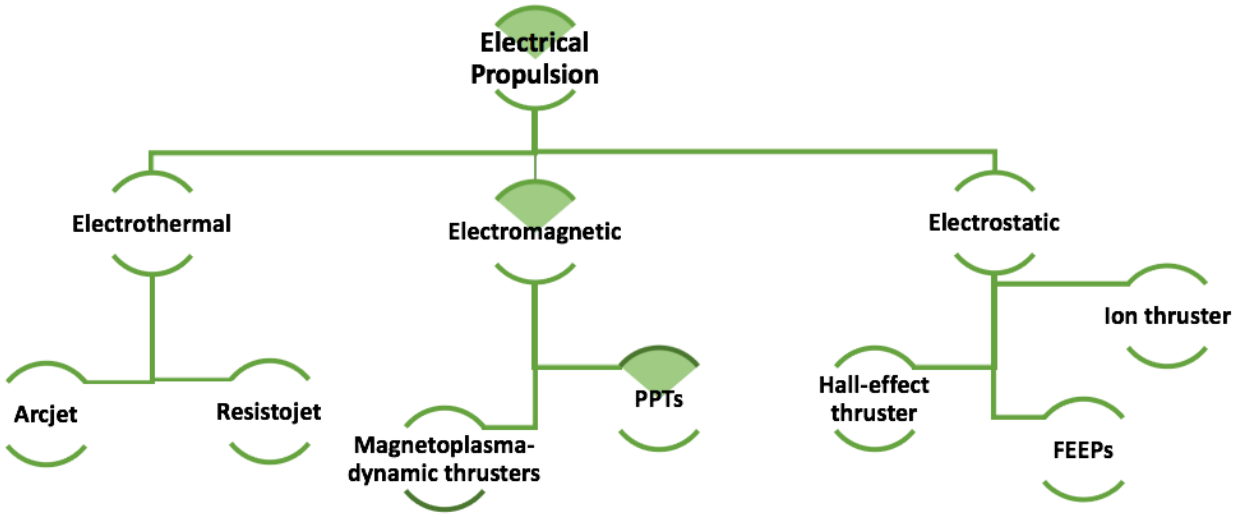

Figure 2: Classification of the main electric propulsion devices

2.2 History of PPTs

The concept of electrical propulsion dates back to the beginning of the XX century, when visionaries from that time not only dreamed but left the concepts to what later on will be the baseline for scientist and engineers into the way to reach the stars. Of course they are the Russian Konstantin Tsiolkovsky and Robert Goddard from the United states, who even living in different geographical positions converged in what today is commonly called, rocket science [3].

Calling back Tsiolkovsky, who was a school teacher and a rocket scientist in his free time, introduced the concept of electrical propulsion in his publication [3] in 1911. At that time, many physicist were working on the development of cathodic rays, and therefore, was not a coincidence that Tsiolkovsky has thought to implement that in his already published rocket equation. The idea was simply to use the cathodic rays to increase the exhaust velocity of the "particles" coming out from the thruster, analogically to the rocket motor where heavy particles are accelerated in the EP Tsiolkovsky was visualizing electrons being accelerated out. Probably this could have been taken as a misunderstood of concepts, due his used of electrons instead of ions but one has to remember that this concepts were stated at the time when the concept of atomic-sized particles was not fully understood. [4] [1]

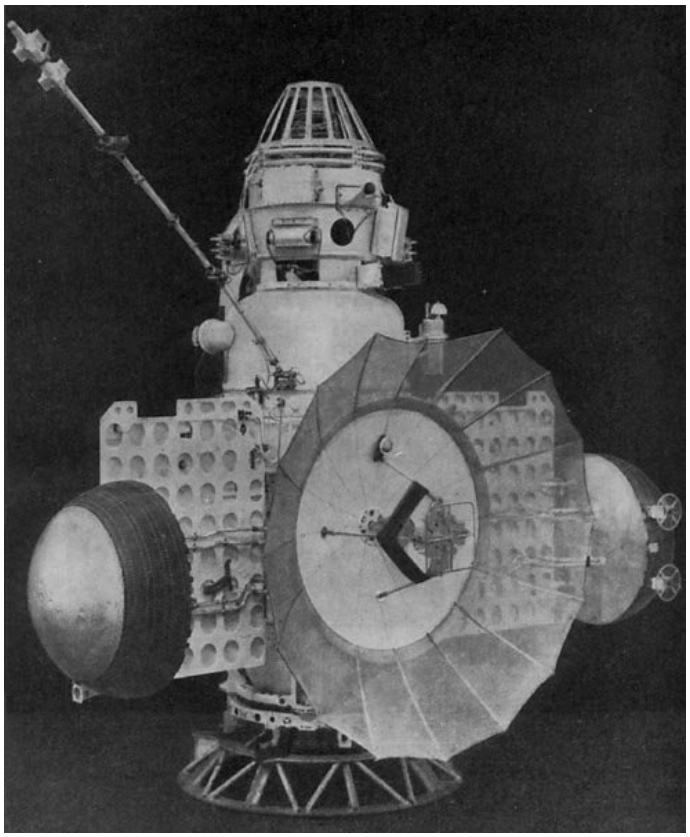

Figure 3: Mars space probe Zond-2 1964- USSR [5]

Meanwhile in the other side of the world, Robert Goddard started working on the concept of electric propulsion since 1907, however, it was not until 19017 when submitted a USA patent titled "Method of and Means for Producing Electrified Jets of Gas" which can be considered the earliest model of an ion engine. [8][1]

Active development of electric propulsion methods start in the 1960's in both the United States and Soviet Union. Design effort was led in the USA by the Glenn Research Center (GRC) and Jet Propulsion Laboratory (JPL) of NASA. Privately operating Hughes Research Laboratories had also significant input. On the Soviet side, the research was divided between a group of research institutes.[9]

In this way, the 30th of November of 1964, the USSR was the first to put a Pulsed Plasma Thruster (PPT) into their Zond-2 probe in direction to Mars (See Figure 3). Although the probe eventually failed due an unclear cause when its communication was lost, it made history of the space flight having the PPTs designed by Antropov and Khabrov, as the first electric propulsion device flown and used in space.[3][9]

Four years later, USA sent its first PPT into space on board the LES-6 satellite, which provided 10 years of service on charge of the attitude control system(ACS), later on in 1971 and 1981, another sets of PPTs were deployed on the missions Synchronous Meteorological Satellite (SMS) and the Navy TRANSIT navigation satellite system, respectively[9].

Since then, PPTs were abandoned due their relatively low efficiency in comparison with their competitors ion thrusters, hall-effect thrusters, resistojets and arcjets, leaving a long history and a vast literature with it. [3]

More recently with the emergence of the CubeSat concept where the use of COTS, an adjective that describes software or hardware products that are ready-made and available for sale, reduces the costs significatly and allows the introduction of research institutions and private sector in which can be known as the new space era. Taking this advantage, the necesity of the traditional systems, now in a miniturized package, carried with it some attempts to bring back PPTs. Can be mentioned as it is the ACDS in Figure 4, designed by Peter Shaw and the Surrey Space center in 2011[10] for the STRaND-1 mission and the already approved by ESA for space flight in 2016, made by Mars Space and Clyde Space[11].

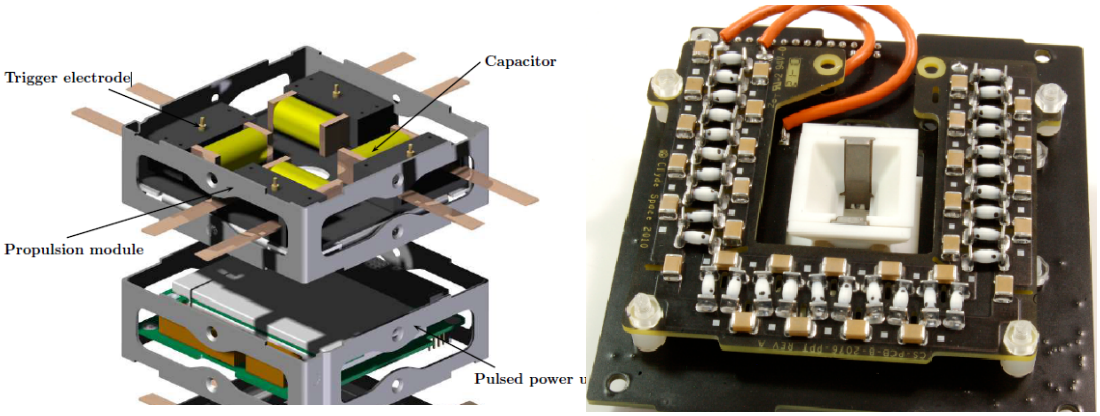

(a) (b)

Figure 4: a) Conceptual design of the PPTs module by Shaw[10] b)Single PPT module for orbit correction by Mars S. and Clyde Space.

2.3 Working Principle

Pulsed Plasma Thrusters are not very different from other means of propulsion when speaking about the role PPU has on them, in fact the PPU in this kind of thrusters makes a difference when talking about performance. This is, because besides to dose the energy to the system, it has to step up the raw voltage coming from the EPS (typically in between 5 to 12 V) in the order of kilo-volts. This order magnitudes makes PPTs to sometimes be avoided due the possible charging potentials it can cause to the surface of the S/C.

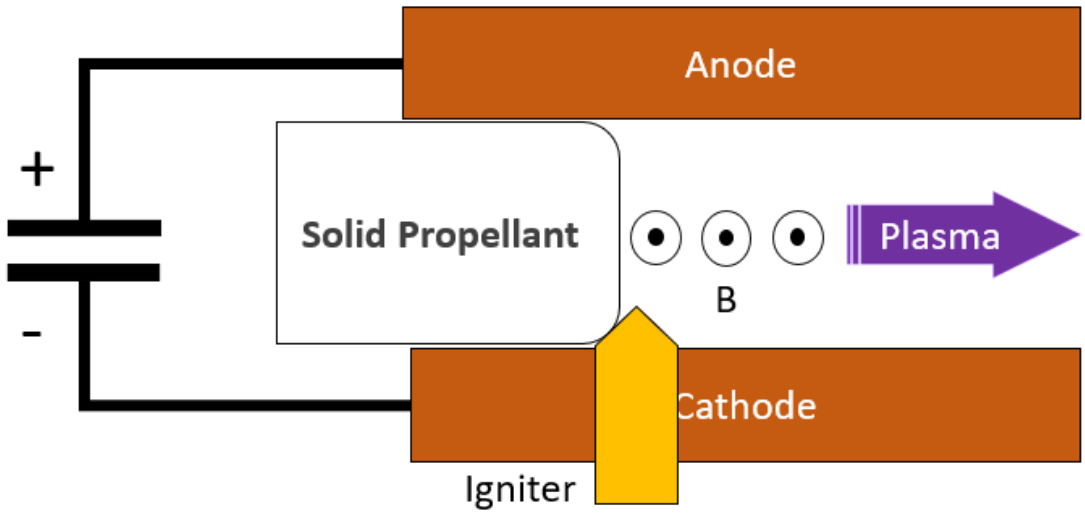

Figure 5: Classic model of a Pulsed Plasma Thruster.

PPTs operate by generating pulsed high current discharges in between a set of electrodes. The electric arc resultant from the discharge, is used to ablates/vaporizes and then ionize the propellant which can be gas, liquid, powder or solid, being this last one the most popular. Thereafter, the ionized propellant is expelled out by the resultant Lorentz force product of the self-generated magnetic field [6]. See Figure5.

Typically this process happens in few microseconds (around 0 and 25) and the behaviour of the plume depends on the mechanical configuration of the discharge chamber which naturally, affects the impulse generated by it. The sequence of the PPT discharge is pictured in Figure 6 where it can be seen how the concept works in a parallel-electrodes configuration.

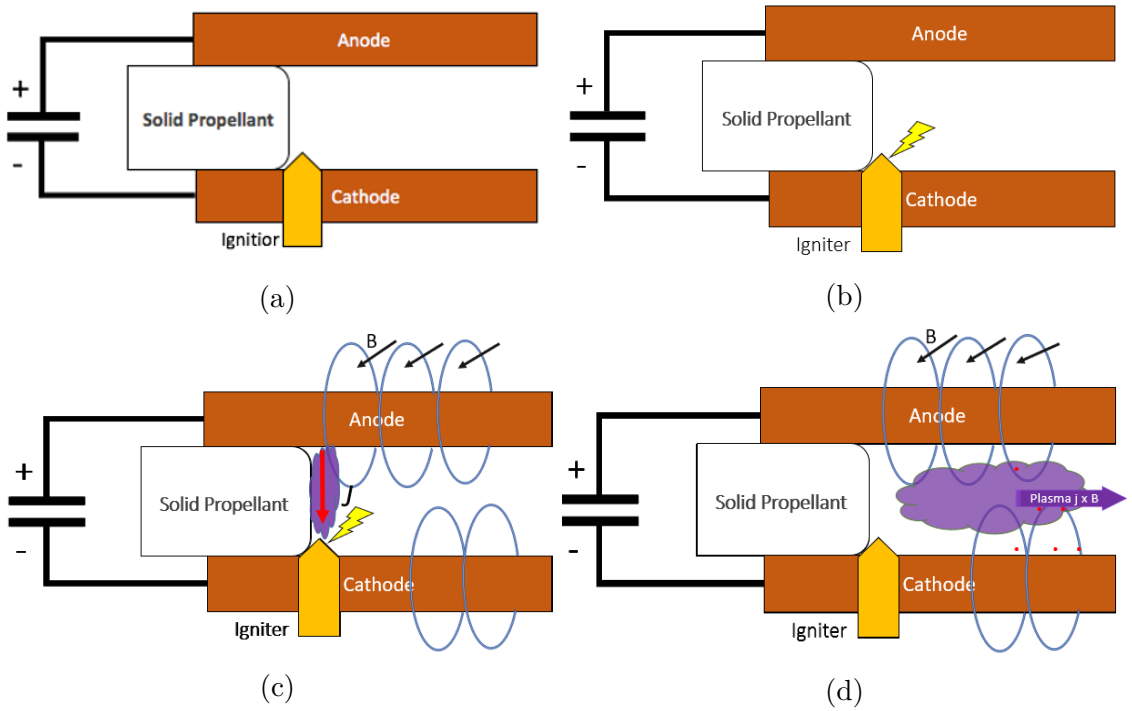

Figure 6: a) Electrodes are charged at the discharge voltage b) The spark is generated by the igniter c) The breakdown is initiated, the propellant gets ablated/vaporized. d) The Lorenz force expels out the plasma with the charged particles product of cross product of the electric field and the magnetic field.

PPT has demonstrated the capability to perform a variety of propulsion tasks delivering an impulse bit ranging from tens of micro N-s to up to 10,000 mN-s and has operated within an energy range of approximately 1–700 J [7].

2.4 Different types of PPTs

By definition, the dielectric strength is considered as the maximum electric field a material can withstand before undergoing into an dielectric breakdown. Overcome this barrier is the main challenge of the igniters in PPTs.

Up to now, there is insufficient study describing the actual mechanisms by which the igniter starts the PPT discharge.Proposed theories include simply providing an initial plasma discharge near the propellant surface. This initial discharge causes sufficient evaporation of the propellant to sustain higher currents. But have been seen in diverse experiments [10] that is possible the discharge even without the propellant, leading more to be the ablation of the sparkplug insulator what facilitates the path to electric current. Alternatively, ultraviolet radiation from the ignition spark can free electrons from the propellant that initiate a discharge along its surface [9].

Within the PPT family, there are different factors that determine the functionality of the thruster. These are mainly classified as how is the spark generated by the igniter and what kind of propellant they use.

This is specially important to due the working principle of the PPTs is based on generating such breakdown in the vacuum of the space where a medium to propagate the electric field is almost non-existent and the dielectric strength goes around 20 -40 kV per millimeter[12].

For this reason, there are several methods for ignition as mentioned in [14][17], being the most common:

- Thermionic emission
- Gap
- Through the surface
- Semiconductors

Thermo-ionic emission

This igniter type works by shooting a pulse of electrons that alters the space charge in the gap, increasing the electric field making ionization more likely and causing the breakdown [15]. This method is not so popular mainly because its necessity of extra drivers and a higher power consumption. Moreover it is more commonly used in gas fed PPTs, due its principle of electron propagation through the gas.

Gap

Gap type are the most common igniters, they are widely present in the automotive industry and its simplicity makes them very attractive. They work by having two electrodes separated by an air gap where the negatively charged electrons on the electrodes are pulled in the direction opposite to the possible positively charged ions until they combine each other creating a path which enables the conduction of the electric current in the form of a thunderous spark.

In air, molecules become ionized in a very high electric field and the air changes from insulator to a conductor, resulting in a standard dielectric strength of 3 kV/mm. For PPTs working a very low pressures as is the vacuum of the space, this dielectric strength increases around 10 to 20 kV per millimeter, making them impractical for μPPTs purposes [12].

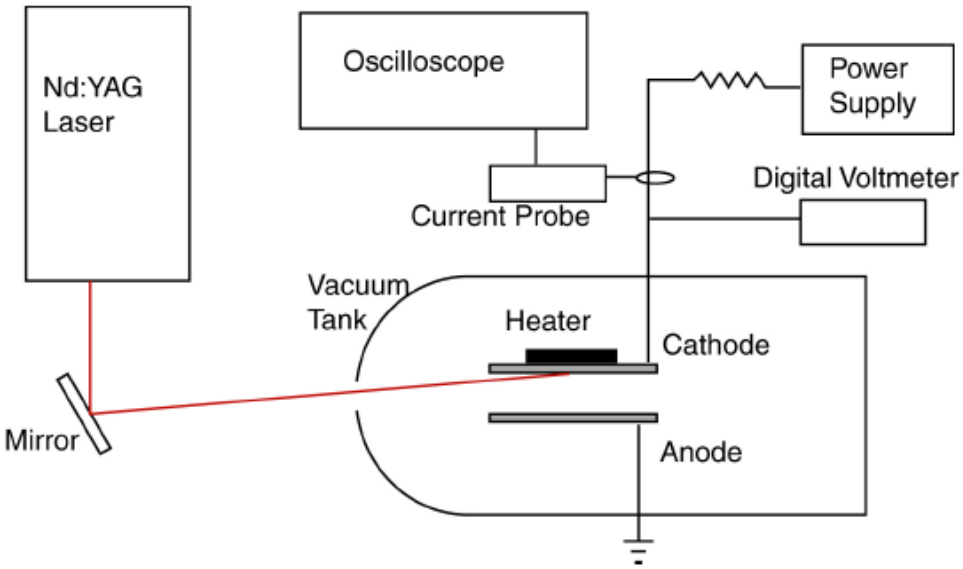

Figure 7: Thermo-laser emission, Princenton.

Through the surface

Through the surface igniters are very similar to gap types, differentiating themselves by the way in how the spark is generated. When, in gap sparkplugs the current has to cross the vacuum in between the electrodes, in through the surface the current travel over the insulator surface that separates both electrodes, decreasing in this way the dielectric breakdown voltage around 5-10 kV per millimeter.

Semiconductors

In semiconductors sparkplugs, the working principle is the same as in through-the-surface with the only difference that along the surface of the insulator, it has a small layer of semiconductor material that reduces the potential needed to trigger the spark. This approach has been well used by Mars Space and Clyde Space in their μPPT system. Although this approach reduces the breakdown to around 3-6 kV per millimeter, it needs a custom-made sparkplug which is considerably expensive for a prototype stage.

Considering the aforementioned ignition methods and because the spark plug is widely considered as important key of the entire PPT due is the component which suffer direct wear during its lifetime, the project moved forward taken the through-the-surface approach considering the manufacturing options available.

Within the propellant side, there is a deeper case of study on the selection of it where the most common are gas PPTs, powder PPTs non- propellant and the ablative thrusters. These last type of thrusters were selected on this work due its

extensive heritage and literature available.

2.5 Argo. Project overview

2.5.1 Previous research

Along the previous research carried out by Odysseus in [17], the baseline was proposed for the PPT's configuration and characteristics that helped to identify the proper PPU for this project. The chosen setup is a compilation of the shape, propellant, geometry, type of ignition and aspect ratio in between the electrodes. The previous is followed listed in the Table 1 :

Parameters	**Chosen configuration**
Propellant	PTFE (Teflon^{TM})
Geometry	Parallel plate electrodes
Shape	Triangular sharped end
Flare angle	15º
Aspect ratio h/w	h=20 w=10
Ignition type	Surface flash-over

Table 1: Selected PPT parameters for ARGO ACS

These parameters were the result of previous tests in a low-energy discharge setup, where a main discharge <1 Joule was achieved [17]. Nevertheless the low energy discharge was demonstrated to be possible but the results were not totally satisfactory at the long run and the the impulse bit was not sufficient to provide a considerable thrust (around 2.21μNs) but worked as a proof of concept and gave valuable information regarding the shape, geometry and propellant used.

After the aforementioned investigation the main body of the PPT was slightly modified, principally to fit a new spark plug design which aimed to bring a better control by triggering the main discharge causing the electric breakdown of the electrical insulator surface in the sparkplug as is appreciated in the Figure 8.

Additionally, the previous investigation pointed the necessity of a reliable PPU due the lack of repeatability the current system had, resulting difficult to determine the real causes of failure. From this point, the present work took as an objective to complete the first functional PPT test bench for its further development. Within the frame of the Argo project was chosen the use of PPTs for attitude control, providing manoeuvrability in the 3 axis of a 3U CubeSat. In order reach this goal, a minimum of a 4-PPTs set is needed while keeping the design modular for its further scalability into 6U or 12U CubeSats.

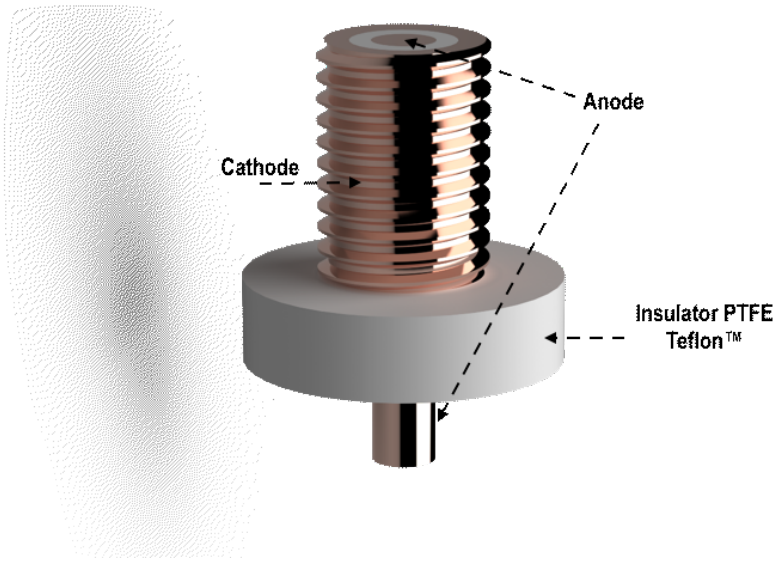

Figure 8: Sparkplug model designed by Odysseus Space

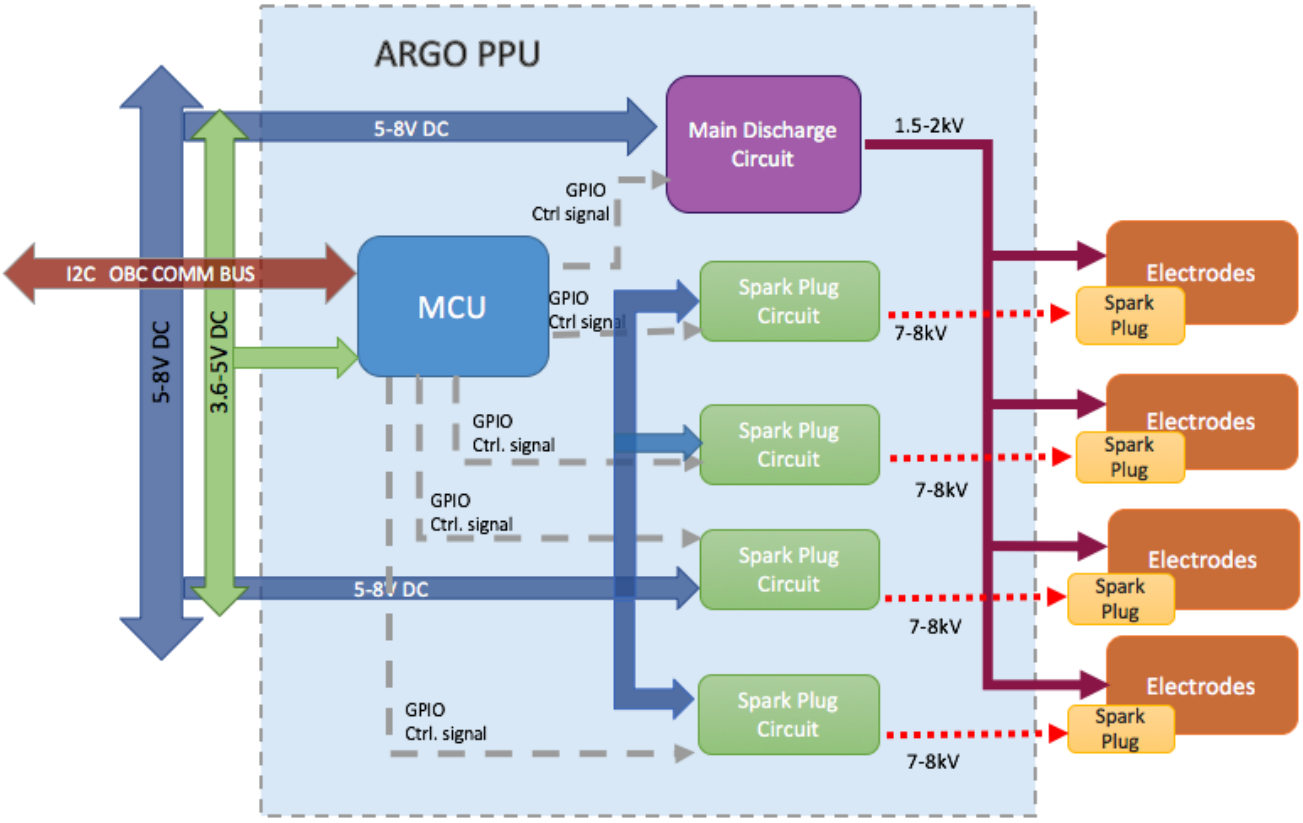

Figure 9: Electric block diagram of the Argo ACS

From this point, the Argo ACS was restructured to meet the development of the engineering model in a period of 7 months. This time was determined by the National

Space Program Office (NSPO) from Taiwan to whom was planned to present the second stage of Argo in order to continue with its development. The system was divided in 2 main parts; the mechanical design which have had considerable progress at this point, leaving the preamble of this investigation and the electrical side, being the PPU which is the main topic of this thesis.

Moreover, due its its modular nature was possible the construction of one SPC instead of the full arrangement of 4 allowing to prioritize the development in a single module.

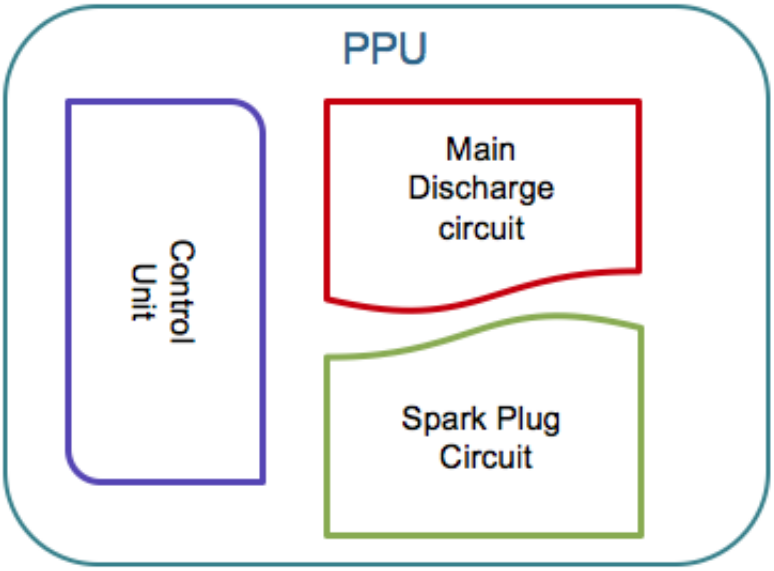

Main discharge circuit
Main discharge circuit which allocates the capacitor bank operating in a 1.5 to 2 kV and delivering 5 J discharge to for ablation and ionization of the propellant.

Sparkplug
High voltage and low current discharge, aiming to overcome the surface dielectric strength of the PTFE in order to reach the flashover and trigger the main discharge in the vacuum of the space.

MCU
Finally, the control is commanded by a microcontroller which main function is to coordinate the discharge of each thruster, manage the power budget by restricting the charge and discharge of the capacitor banks and keep the contact with the OBC.

Thereby the following chapters of this manuscript are focused to the development of each subsystem.

3 Main discharge circuit

As a concept, a propulsion system is a machine that produce thrust, which working principle is based on the Newton's third law of motion. For every action there is an equal and opposite reaction. In any propulsion system, a working fluid is accelerated by the system and the reaction to this acceleration produces a force that is proportional to the mass flow and the exit velocity. In PPTs this is possible due the ejection of charged particles as plasma throughout the electrodes due the Lorenz force. To achieve this, a relatively high amount of energy is discharged in a small fraction of time in the order of milliseconds. This energy is stored in a particular section known as the main discharge circuit, which consist in an bank of capacitors triggered by an ignitor in a determined fashion[44].

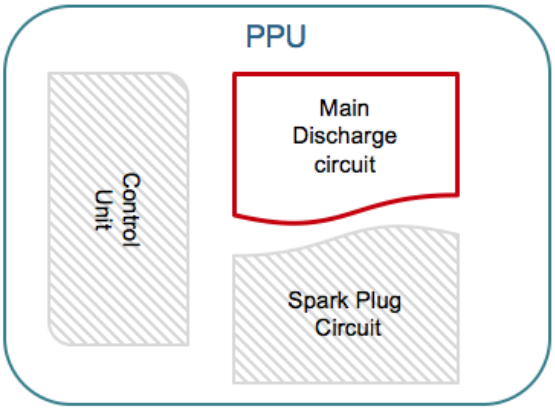

Figure 10: PPU:Main discharge circuit

3.1 Early analysis

Following the guideline of Odysseus Argo project, a previous study was carried out before the start of this work, where a low energy PPT was presented. In this investigation [17] was studied the performance of a 1 Joule energy PPT. The author used a capacitor arrangement composed by two strings of capacitors in parallel, each one rated at 0.5 μF and 700 V, resulting in a total capacitance of 1 μF at 1400 V storing a theoretical maximum of 0.98 *J*.

One of the issues observed, was the increasing rate of misfires after few thousands discharges. Is believed the increasing of discharge energy helps to decrease the carbon coating formation on the electrodes, thereby prolonging the life time of the system.

In base of the aforementioned work, new ideas have been planted and an energy of 5 Joules have been chosen with an operational voltage in between 1500-2000 Volts. At this working conditions, can be calculated the capacitance needed to reach such energy. This can be done directly from the equation

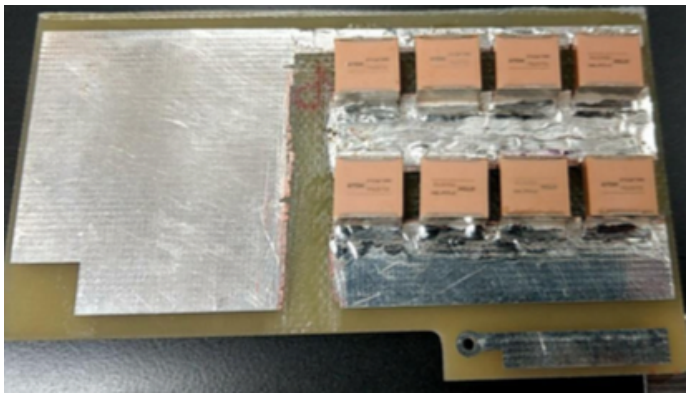

Figure 11: Previuos low energy capacitor bank[17]

$$E = \frac{1}{2}CV^2, \tag{1}$$

where C stands for the value of the capacitance in Farads, V for operational voltage in Volts and E for the energy in Joules.

From the derivation of this equation we get

$$C = \frac{2E}{V^2} \tag{2}$$

substituting

$$C = \frac{2 \cdot 5}{2000^2} = 2.5\mu F. \tag{3}$$

This is the capacitance needed to achieve the desired energy.

Next step was to define the charging rate of the capacitor. By formula this is defined as:

$$t = 5RC, \tag{4}$$

where R stands for resistance in Ohms, C for the capacitance in Farads and t is the time in seconds.

This $5RC$, is the theoretical 100% of the charging voltage. Nevertheless, to understand the capacitor charging and discharging process is important to know that it is not a linear function.

It can be seen in Figure 12 that, at the period of time 1 T the electrons transfer rate is faster and decreasing as the potential in the capacitor get closer to the charging voltage. This is because the charging rate follows an exponential function given as:

$$V_c = V_s(1 - e^{-t/RC}), \tag{5}$$

where each T represents the 63.2% of the remaining charging voltage at each point.

Theoretically, after a period equivalent to 4 time constants (4T), the capacitor is virtually fully charged and the voltage across the capacitor is approximately 98% Vs. This time period is known as *Transient period.*

Once the voltage is equal to the charging voltage (5T), the incoming current is equal to 0 and the capacitor behaves as an open circuit. This point is known as the *Steady state period.*

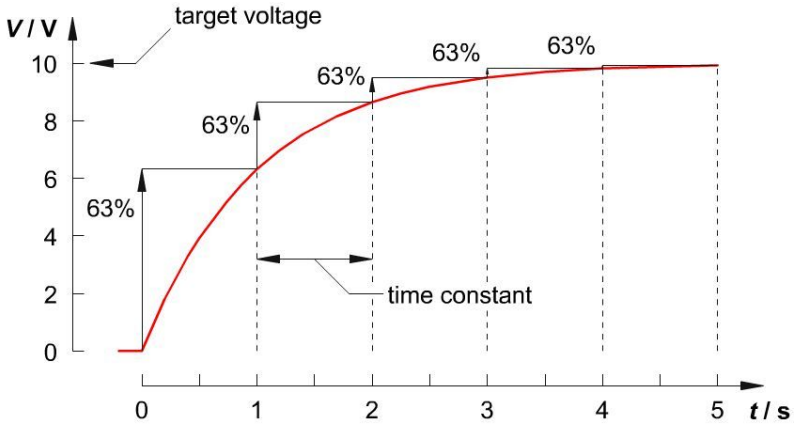

Figure 12: Capacitor charging rate

It is particularly important because it will define the firing frequency and the energy at any moment. This can be better understood from the Table 2.

Time constant	Percentage of maximum Voltage
1T= 1RC	39.3%
2T= 2RC	86.2%
3T= 3RC	95.0%
4T= 4RC	98.2%
5T= 5RC	99.3%

Table 2: RC charging table

Considering the aforementioned, the selection of a suitable resistor was made. It should deliver a reasonable charging time for the capacitor bank because, after all, it will define the maximum frequency at which the PPT can be operated and the power drawn from the power unit of the satellite.

As all experiments were done in the Combustion Lab from the Aeronautics department facilities in NCKU, the power supply available was a MATSUSADA ES-5R1.2-2G rated at 5 kV at a maximum delivering power of 5 W. Hence, following the Ohm's law, we derived :

$$I = \frac{P}{V} = \frac{5}{2000} = 2.5\ mA, \tag{6}$$

where 2.5 mA is the maximum current the power supply can deliver. Therefore, a suitable resistor must be

$$R = \frac{V}{I} = \frac{2000}{2.5 \cdot 10^{-3}} = 800 \ k\Omega. \tag{7}$$

After to look in the repository the closest value available was and arrangement of 2 resistors of 470 kΩ each one, giving a total series resistor of 940 kΩ. Which is the value used for next calculations.

In accordance with the Equation 4, this resistor value, at 5T will represent a charging time of :

$$t = 5 \cdot 940000 \cdot 2.5E - 6 = 11.8 \ sec. \tag{8}$$

For safety reasons at the moment to manipulate the board, the use of a *Bleed resistor* is necessary. A *bleed resistor* is an extra resistor with the only purpose of discharge the capacitor in a certain amount of time. Using the Equation 4 can be calculated the time the capacitor bank will take to discharge. At the same time, due the resistor is placed in parallel to the capacitor and in series with the charging resistor, it produce an undesired voltage divider, which will decrease our charging voltage, and of course this represents a power loss.

A voltage divider is a basic configuration used when from an input potential (V_{in}) is desired to take an output voltage (V_{out}) which is a proportional fraction of the input. The output voltage can be derived from the equation:

$$V_o = \frac{V_i \cdot R_2}{R_2 + R_1}. \tag{9}$$

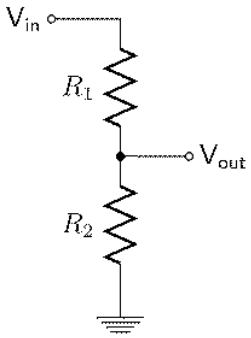

Figure 13: Simple voltage divider.

A suitable resistor was selected in order to have as less looses as possible, but at the same time do not have the necessity to wait too long to handle the circuit in case that is needed during the tests. So, deriving the Equation 9 results:

$$R_2 = \frac{V_o \cdot R_1}{V_i + V_o} = \frac{1950 \cdot 940}{2000 \cdot 1950} = 36.6 \ M\Omega. \tag{10}$$

Due the availability of the resistor, a 50 MΩ was chosen, representing an increase of only 13 volts at V_o.
Once all the values were calculated, the simulation was performed. On the schematics from the Figure 14 is shown the basic diagram of the circuit. Something that has to be mentioned is the fact to have used an inductance to simulate the PPT's electrodes. This came from the inherent plasma properties and also observed in [22] where the plasma created in between the electrodes at the moment of discharge, electrically behaves as a very small inductance in the order of μH.

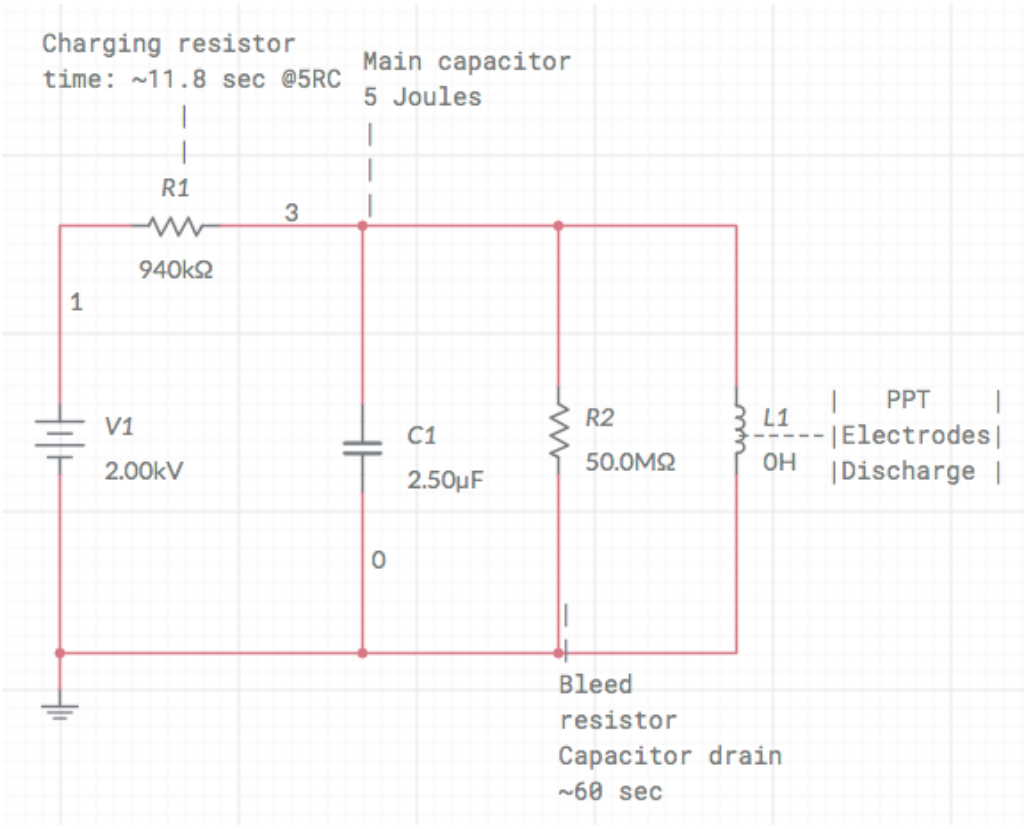

Figure 14: Schematic for the Main discharge circuit.

3.2 Testing and validation

Consequently the commercial components suitable for working at vacuum environment were selected.

Find capacitors at 2.5 μF and rated at 2000 V was not a simple task. Usually the capacitors suitable to work at vacuum conditions are ceramics. This kind offers a wide variety of capacitances and voltage rating. However, capacitors rated at higher voltage usually have capacitances in the range of nano Farads. After to look into the available options, was found an array of ceramic capacitors from EPCOS(TDK) in

package of 10 capacitors in parallel of 1μF each one rated at 500 V and an operating temperature -55 to 125°C. Therefore, to reach a maximum voltage of 2000 V was necessary to stack them in series, getting a total capacitance of 2.5 μF at 2000 V.

Due the relatively small amount of components used for this circuit, the prototyping process was very quick. But the low expertise working at such high tensions, was decided to run out all the necessary precautions.

Thereby, it were soldered the capacitors on the uncoated side of the board. This with the idea to minimize the risk of flash-over on the board surface.

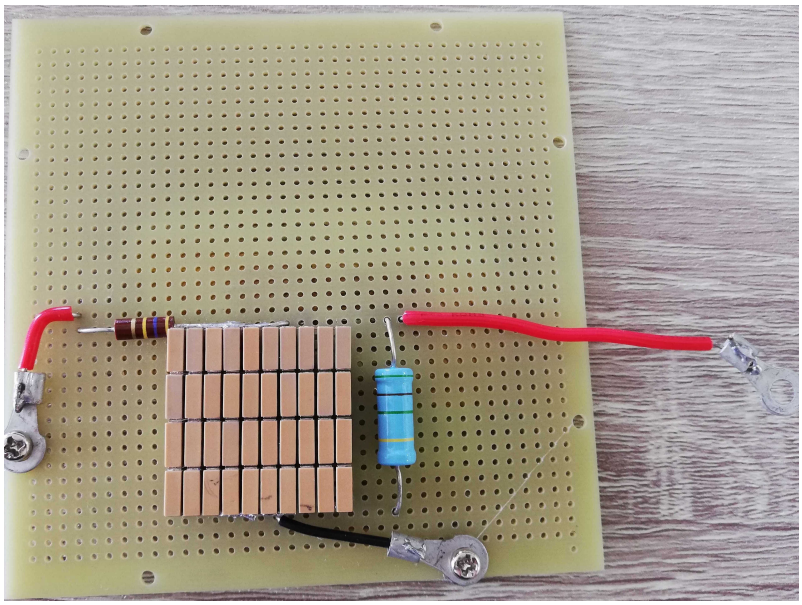

Figure 15: PPU: Main discharge circuit breadboard.

For the input and output connections were used ring connectors with M3 bolts and nuts with the purpose to make it robust and give a wide gap in between ports to avoid potential breakdowns.

Testing

The simplicity and functionality of the circuit made the testing going very smooth. The capacitor bank was in overall, tested for around 100,000 discharges without presenting any physical or electrical wear. These discharges were performed along this work and are better described in the following chapters.

3.3 Final design

After have overcame more than 20,000 discharges, the circuit was mature enough to be designed for manufacturing. Even when the previous version fulfill the necessities of a *proof of concept* stage, for the final version some other characteristics had to be

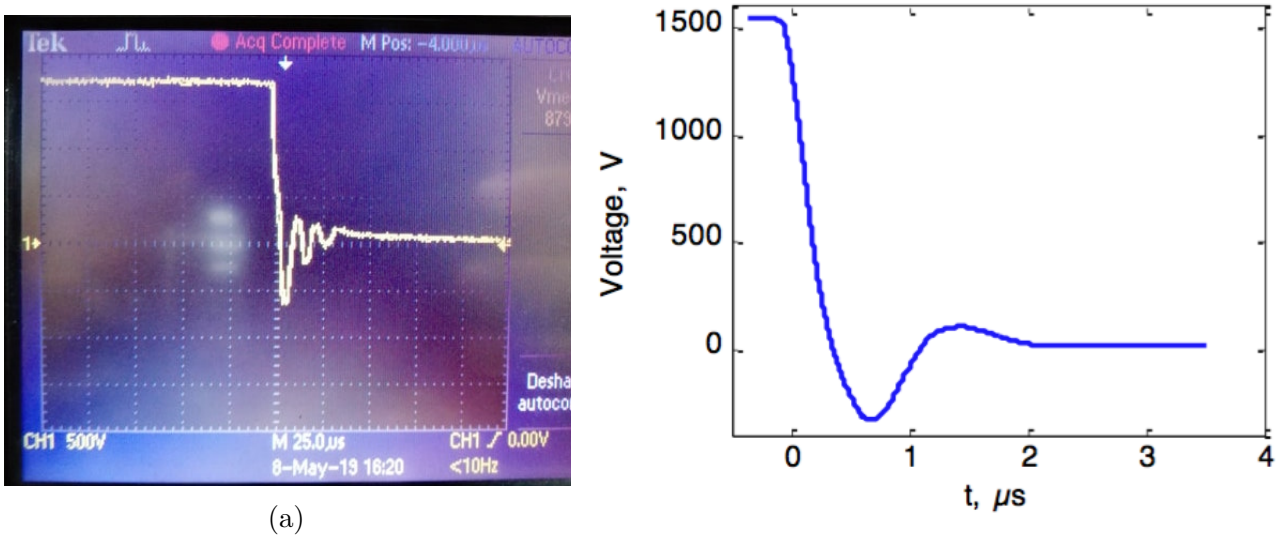

(a) (b)

Figure 16: a) Discharge of the developed prototype at 1700 V and 3.62 Joules. b)Characteristic discharge of the capacitor bank in PPts[13].

considered.

First of all a DC-HVDC converter has to be chosen. For the task the use of 4 DC-DC converters EMCO AG20 was chosen. They are reliable converters able to step up voltages in DC from 5 V up to 2000 V with an maximum output current of 0.5 mA and an average power consumption of 1.6 W per unit. Moreover they offer a controllable linear output by varying the voltage in the control pin by software using PWM.

Within the design considerations were evaluated the current space available and the chance to provide a fast charging by switching on the HVDC converters, otherwise turning them off and operate only with one for lower the power consumption to 1.6 W.

Finally, a *bleed resistor* of 50 MΩ was included for safety reasons during the campaign tests.

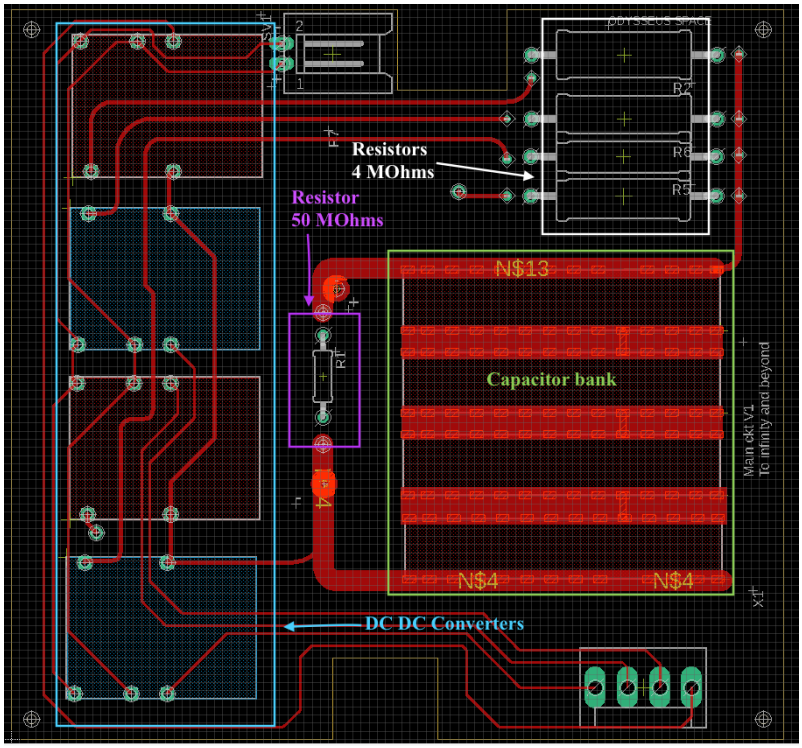

Figure 17: Main discharge circuit layout, final design.

4 Spark Plug Circuit

One of the central components in such micro-PPT is the igniter subsystem, which is required for creation of the flash-over plasma and initiation of the main discharge. There are several methods to provide the ignition of the main discharge in vacuum, however, to provide a reliable, compact and robust ignition with a reasonable life time (about 1E6 discharges) is still a challenge.

In this section are evaluated the possible solutions for having a reliable electronic circuit from their theoretical analysis to the prototyping and testing.

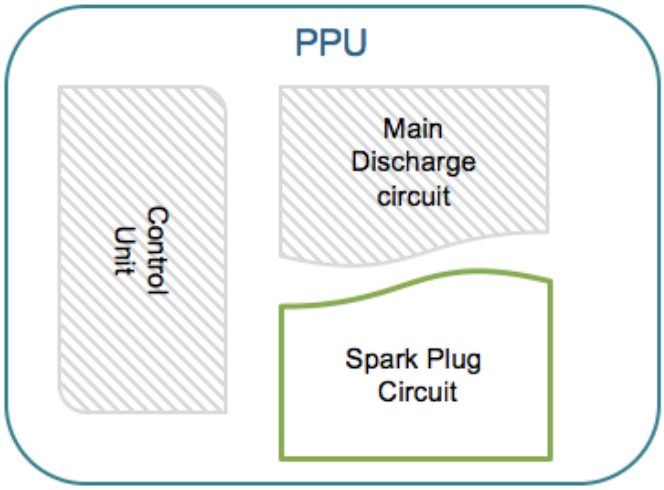

Figure 18: Spark plug.

4.1 Early analysis

Being the SP circuit one of the main reasons of failure in PPT's, was decided to keep the work flow as simple as possible. Hence, it was decided to start the experiments in which seemed, the easiest approach to the most elaborated.

An deep investigation was carried by the author of this work on this special subsystem because according to literature[10][18][19][21], is the most likely system to fail. This is, mainly because the life time of the components and the carbon coating formation around the electrodes altering the breakdown voltage necessary to reach the spark in vacuum, affecting directly the reliability of the system response.

Several solutions have been thought about how to discharge a controlled pulse of high voltage withing such small space. Taking in consideration the heritage from literature and the aims of the project, some of them are listed below:

They have been classified in groups according the voltages at which there are handled because after all, this is one of the biggest concerns due the danger of flash-overs within the circuitry.

Low voltage input	High voltage input	Other
1) Inductance/ Coupled inductance	~~3) Mechanical trigger~~	~~6) Thermo-ionic emission~~
2) Dc-Ac-Dc voltage multiplier	4) Reed Relay switch	
	~~5) High voltage transistor~~	

Table 3: Identification of possible solutions.

After the discussion of all the possible approaches, some of the options have been already discarded. The reason is because they resulted unsuitable for the target application, as is Thermo-ionic emission. In the case of the mechanical trigger, facts as mechanical fatigue and arc welding are some of the main concerns, moreover from previous work[10], have been faced problems at the moment to design a reliable mechanism to induce the sparks and even when one of the cleanest solutions could be the use of electronic switches as the case of the high voltage transistor, the IXYL60N450 IGBT was the highly rated transistor available in the market and it is up to 4500 V only.

In this way was organized from the simplest and cheapest option the remaining options, being

1. Reed Relay switch
2. Dc-Ac-Dc voltage multiplier
3. Inductance/ Coupled inductance

4.2 Reed relay switch

One of the most important considerations in any design is to keep the lowest number of components as simple as possible. Following this logic, the use of a simple electro-mechanical switch seemed to be a straightforward alternative for the purposes of the Argo Project.

It consist on a switch activated by inducing current into a coil creating a magnetic field and closing the contacts as is shown on the Figure 19a. This reed relay seemed to be the suitable alternative for the aim of the project because it offers insulation between the logic and the power circuits, keeping the switch contacts in a vacuum tube inside its package.

The relay chosen is the DAT70515F-HR from Cynergy 3, rated at 10,000 VDC and a maximum current of 3 Amps controlled by a 5 V coil with a mechanical response time of 5 ms.

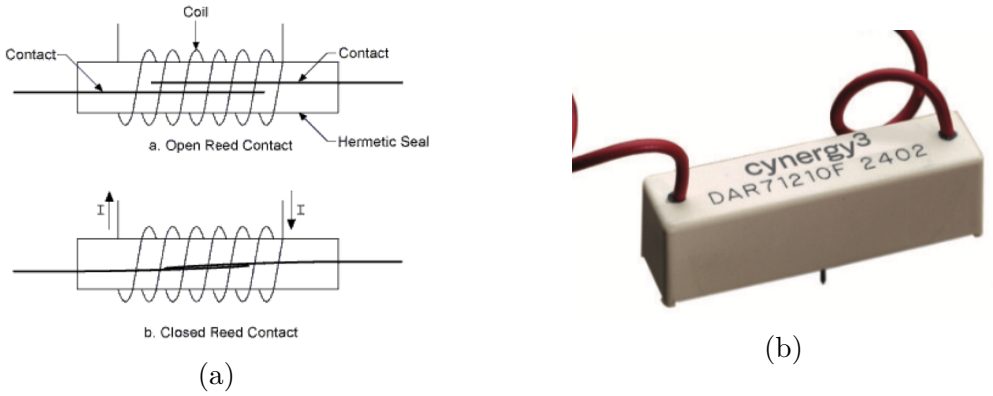

(a) (b)

Figure 19: a) Reed relay mechanism. b)D-HR Cynergy3 10,000 VDC.

As it is well known from previous experiments [18], one of the major problems is the carbon coating formed around the spark plug electrodes and the heating on the insulator due high current going through it. Have been seen how the coating effect can be diminished by using a high energy discharge at the ignition. Typically the energy range is in between 0 to 0.1 Joules, so that, a higher energy was aimed for this project.

An array of 8 capacitors HV2225Y332KXMATHV from Vishay Vitramon was chosen. Their selection was based on the high working voltage and their versatility to form different configurations if needed. Each of them is rated at 5,000 V and 3,300 pF. They were settled in an array consisted by 2 strings in series each of one with 4 capacitors in parallel. Where the total capacitance can be calculated by:

Capacitance

$$\begin{aligned} C_{tot} &= C_1 + C_2 + C3 + C_4 \\ C_{tot} &= 3300 + 3300 + 3300 + 3300 \\ C_{tot} &= 13200\ pF \end{aligned} \tag{11}$$

Considering the 2 strings are in series:

$$\begin{aligned} C_{tot} &= \frac{13200}{2} \\ C_{tot} &= 6600\ pF. \end{aligned} \tag{12}$$

From the Equation 1 at an operational voltage of 8 kV the equivalent energy would be:

$$\begin{aligned} E &= 6600 \cdot 10^{-12} \cdot 5000^2 \cdot 0.5 \\ E &= 0.206\ Joules. \end{aligned} \tag{13}$$

Furthermore, a set of resistors had to be chosen. They were divided on the charge and discharge resistors. Both are directly related by the equation 4 where the time was intended to be as short as possible. The purpose of these resistors is to protect the power supply from possible fly-back currents and the reed relay respectively to be burned by the high instantaneous current coming from the capacitors.

The charging resistor, was chosen at 100 kΩ giving a charging time of 3.3 ms at 5 *RC*. On the other hand, the discharging resistor was chosen in order to protect the maximum allowed current through the relay. Following the same logic, at 5 RC the minimum suitable resistor for 8 kV should be 5.3 kΩ limiting in this way the current to 1.5 Amperes. However, is known the capacitors discharge current operates at large electric current(10's Amperes), bringing a new concern about the properties of the resistors to withstand such high current even for a short period of time.

This new concern led to not only pick the appropriate current limit but to double check the properties of the components required for such application. In this way, High pulse load carbon film resistors from Vishay were chosen. These resistors are used for the automotive and medical sector and according to data sheet they can withstand pulses up to 100 W for a maximum of 10 ms without being damaged. Thereby, 1 MΩ CMB0207 resistors were selected, handling a theoretical maximum of 64 Watts with a discharge time of 31 ms (Equation 4).

From Figure 20 can be observed that one of the advantages of this topology is its straight forward and scalable configuration. Where S1 represents the Reed Relay connected to the Spark Plug electrodes, R1 the charging resistor, R2 the discharging resistor and C1-C8 the capacitor bank. Although the proposed circuit was built for only one spark plug, it can be seen how the concept can be easily scaled up.

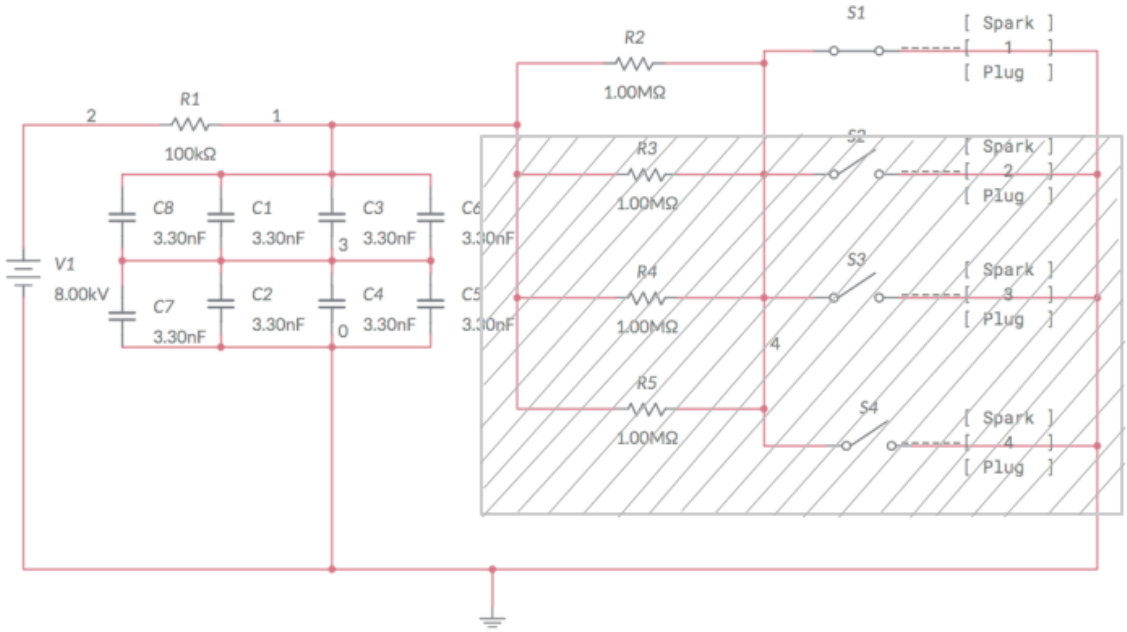

Figure 20: Proposed topology for the reed relay circuit.

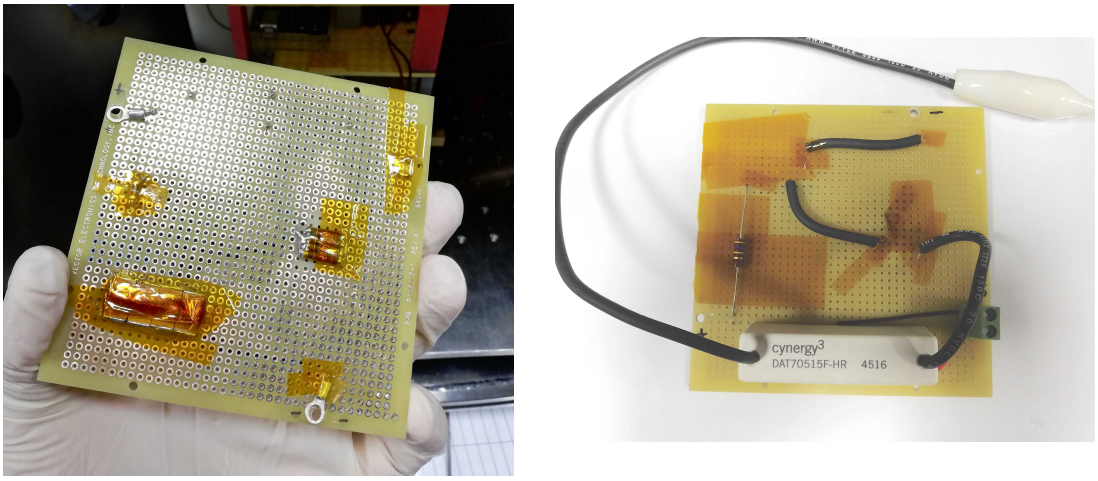

Figure 21: Reed relay circuit.

4.2.1 Testing and validation

Test 1

After have been soldered, the circuit was placed outside the vacuum chamber and connected the input voltage to the power supply and the output to the spark plug electrodes. To control the discharge a simple routine was carried in an Arduino Uno and wired directly to the relay control coil. As it was the first attempt, it was decided to not plug the main discharge circuit to the PPT electrodes until first have a controlled spark.

Once everything was wired, the tests begun and the first issues were faced. During the charging process the circuit started discharging without being triggered by the control but no clear sparks were observed and the power supply was shutted down on every time it reach a voltage around 4 kV. It was thought to be a board flash-over problem so, it was decided to place the board into the vacuum chamber and run the test again.

At this time, the vacuum chamber from the NCKU ZAP Lab was working relatively well and used to take around 1 to 2 hours to pump out the air and reach a vacuum of $5 \cdot 10^{-5}$ Torr.

The experiment was restarted and the results were not different. The power source automatically shutted down in between 3.5 and 4 kV. The problem was thought to come from the soldering pads on the circuit board. So they were sanded down and the components were covered with Kapton tape as it is shown in Figure 21. The circuit was tested again, this time a dim spark was seen around the charging resistor R1. For this reason, the resistor R1 was replaced by a 470 kΩ *through the hole* resistor with the idea to increase the space in between the terminals and avoid a flashover in between them. This did not completely work because the power supply was still shutting itself down after the first test.

Therefore, the capacitors were wrapped in Kapton tape and the charging resistor was changed to 5 MΩ as it was thought the capacitors could be drawing too much current from the power supply and it was the cause of the constant rebooting. Now with the implementation of the new resistor, the power drawn from the supply was limited to 5 Watts.

Nevertheless, the problem was not solved and the capacitors were taken away from the board and tested only with the resistor in series, wired by a high voltage cable. The purpose of such experiment was to discard a problem caused by the mounting on the breadboard. As it kept presenting the same behavior, the experiments were stopped and was determined the problem was coming from the HV power supply.

Test 2

In this new set of experiments a new high voltage power source was needed. Thus was decided to continue the investigation to the next approach for the generation of the high potential needed. For practical purposes, a circuit from a "mosquito zapper" was recycled due its low cost and quick availability. It is a simple circuit which in principle is a DC-AC-DC voltage multiplier. It is described in the next section of this manuscript but for purpose of the current experiment it was used as continuous high voltage supplier. It delivered 5 kV DC going directly through the reed relay switch to the spark plug electrodes.

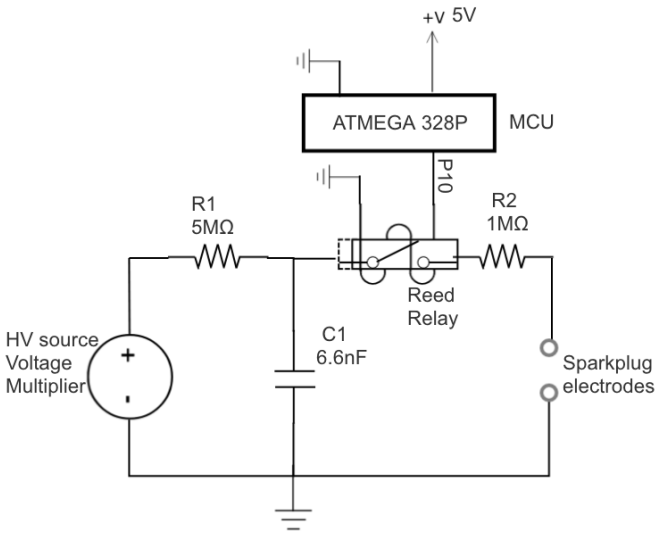

Figure 22: Reed Relay circuit schematics.

The circuit was wired and tested with the new power supply in vacuum. Nevertheless, the circuit was unable to produce the discharge on the sparkplug. The first idea was that the voltage was not enough to overcome the dielectric strength on vacuum. Following this idea, the circuit was taken out the chamber and tested in atmosphere to ensure there was not any wiring problem. As a result, several sparks were seen in between the capacitor bank and the test was stopped. This happened because the high potential and incorrect isolation of the capacitor terminals broke the dielectric strength of the air and causing a corona.

One more time and after ensuring the connections and the health of the capacitors, the circuit was placed again inside the vacuum chamber and tested without any success. Due all the experiments were carried inside the vacuum chamber, it was impossible to measure the discharge rate of the capacitors and in this way isolate the problem in an specific section. Thereby it was thought, the resistors protecting the relay were indeed slowing down the current necessary to produce the ignition on the electrodes and they were removed.

Consequently, the circuit was tested and finally the sparks were generated. Nevertheless after few discharges the reed relay started presenting issues where the CLOSE state was kept for longer than commanded by the microcontroller. In principle was thought the problem was caused due a possible magnetizing of the internal switch terminals so, the experiment was repeated shortening the pulsed length to 70 ms, 50 ms and 30 ms obtaining the same results. The tests were concluded after the total malfunction of the relay where the internal plates got stick closed.

After 2 weeks in the laboratory and with the aforementioned evidence, the use of this topology as ignition control was discarded, leading the course of the project to continue with the next approach proposed in the early analysis of this chapter.

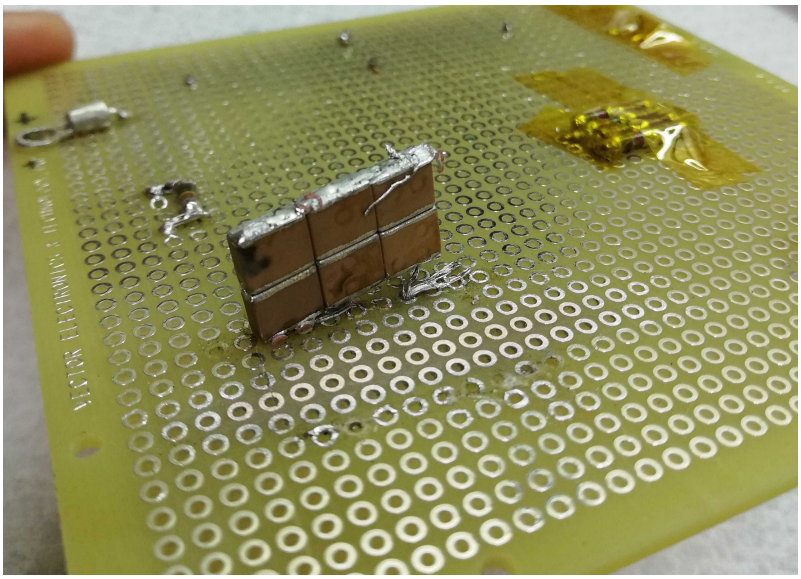

Figure 23: Capacitor bank after the electric arc between them.

4.3 Cockcroft-Walton Voltage Multiplier

After the first attempt did not succeed, the next approach (Table 3) was to continue with the voltage multiplier. In substance it was the next simplest solution, even though the numerous components it requires.

Cockcroft-Walton voltage multiplier is a configuration allegedly invented and used for first time by Sir Cockcroft and Walton in 1932 to power their particle accelerator at Glasgow University[42]. At that time, it made use of large scale selenium rectifiers used as diodes. Nowadays, it uses a set of capacitors and diodes to multiply and rectify an AC signal into DC.

Therefore and despite the variety of voltage multipliers, this topology was selected for its simplistic concept. This section will focus on explain its working principle by splitting the C-WVM in 3 different levels.

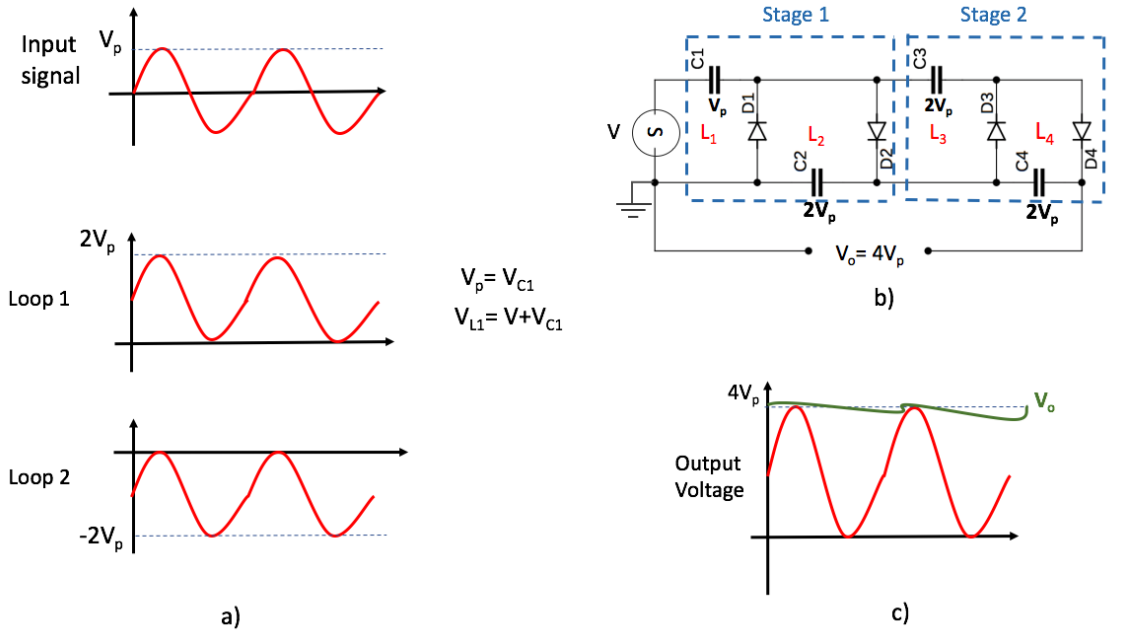

Figure 24: a) Clamper behavior in each loop. b) C-WVM of 2 stages of doubler circuits. c) Signal at the output. Green signal is with a load due the constant charge and discharge of the capacitors while the red waveform is the signal amplified at its output by 4 Vp

- Clampers.- A clamper circuit is a configuration that fix in either positive or the negative the peak of a signal. It does not work by limiting the peak-to-peak amplitude but instead, it shifts all the waveform up or down its reference level.
- Voltage doubler.- The voltage doubler configuration consist of two clampers in series which double the magnitude of the signal by the reason of $V_o = 2V_p$,

where V is the amplitude of the input voltage [23]. Basically it works by adding on the shifted amplitude of the input waveform stored in the capacitors at each stage.

- C-WVM.- Essentially, it is an extended version of a voltage doubler circuit. Usually this topology is divided in stages, where each one is composed by a voltage doubler circuit and the output voltage is taken from the input of the first stage and the output of the last one as showed in Figure 24.

Also in the Figure 24 can be seen how for each loop of the voltage multiplier the signal is transferred to either the positive or negative cycle of V, charging the capacitors at $2V_p$ except for the first one. This is because although the voltage reflected at the first loop is $2V_{ip}$, it is produced by the addition of $V_{ip} + V_{C1}$.

Due the C-WVM only works amplifying AC signals, was necessary to make use of a circuit to convert the 5 V DC from the satellite's battery to AC. Also in the searching of a high voltage source to power up the reed relay in the section **3.3**, the first approach was a circuit taken from a *"Mosquito zapper"*, which was a cheap and easy solution. This circuit is commonly known as *Joule Thief* because it is capable of draw all the energy from a battery even when its voltage has decayed due the decrease of current. It works by *hooking* together two poles from two inductances, usually a set of winded cables around a ferrite coil. At the same time, they are connected to a PNP bipolar transistor (BJT) which in substance, acts as a switch commuting the flow of current in between the 2 inductances, stepping up the input voltage V_{in}.

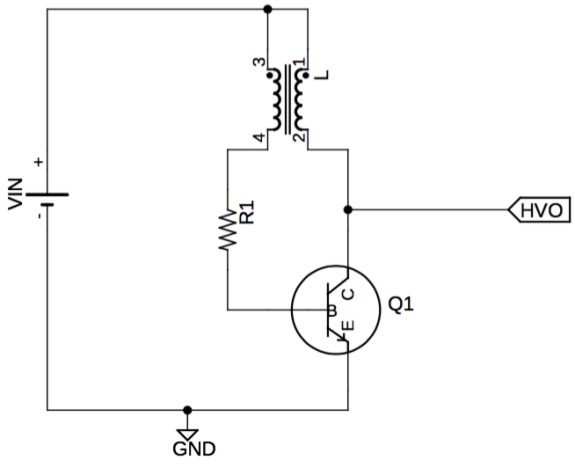

Figure 25: Joule thief simplified schematic.

Even when the Joule thief taken from the circuit was a good approach to convert DC into AC, it was limited by the manufacturer to the purpose it was designed for and by itself reached only 2 kV peak without the possibility to modulate its output.

Despite it worked good enough to reach 8 kV DC at the output, it did not show the expected behavior since 6 stages had been used and in optimal conditions and with this number of stages the voltage must be significantly higher.
Nevertheless, once that reed relay configuration failed, the C-WVM changed to be the main priority of the project and consequently more time was dedicated to its study.

4.3.1 Testing and validation

Test 1

As aforementioned, after have had discarded the reed relay configuration, the C-WVM should be redesigned for its use as main trigger of the ignition in the sparkplug. For this reason some characteristics had to be reviewed for its adaptation to the new objective:

- Direct control of the ignition through the C-WVM.
- Capacitor bank of 0.2 Joules.
- In order to easily detect any failure, has been thought to make the circuit modular, dividing it into 3 sub-circuits.
- Use of *through the hole* components to facilitate the prototyping.

Therefore, the first action was to migrate the *zapper circuit* into a new board and opening a port for its control by the MCU. In Figures 26 and 27 can be seen how a BJT and its base resistor were added. Using the BJT in its saturation region allowing to used it as a logic switch.

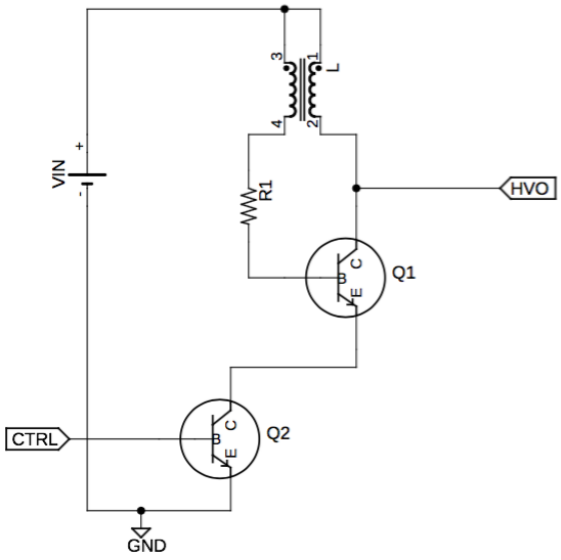

Figure 26: Modified Joule thief for its control using a BJT 2N2222 in Q2

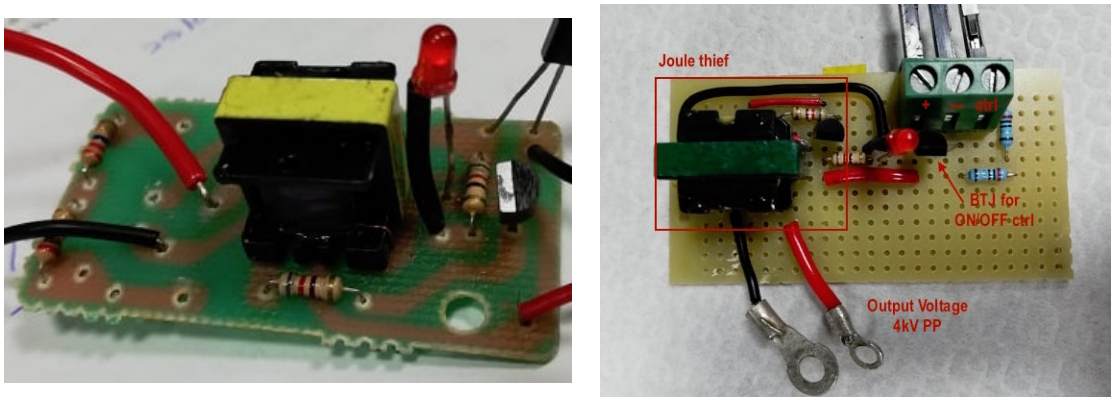

(a) (b)

Figure 27: a) Joule thief taken from the *"zapper circuit"* b) Joule thief re-designed in a breadboard.

The next step was to build the capacitor bank. For the C-WVM, the capacitor bank across the load input becomes an important part of it because, besides of storage the energy to be released for the spark, it provides a DC rectification instead only an offset DC signal at the output and its value only affects the time of the transient response [24]. As it was planned, to simplify the prototyping was proposed the use of *through the hole* components and the capacitors were bought in a local electronic shop, so that, the variety of components was limited. The most suitable capacitor found was a ceramic capacitor rated at 2 kV and 22 nF.

At this conditions and expecting a peak voltage of 8 kV, it was required to use an array of 5 capacitors in series, allowing a maximum voltage of 10 kV. As the capacitance in this configuration follows the reason $C_T = 1/(1/C_1 + 1/C_2 + 1/C_3...)$, the total capacitance resulted 4.4 nF. Thereby, a second array of 5 capacitors was added to double its value. In this way an array of 10 capacitors, arranged in 2 rows in parallel of 5 capacitors in series, provided a total capacitance of 8.8 nF. The array was soldered onto the breadboard giving a maximum theoretical energy of 0.28 J at 8 kV(Figure28).

Consequently, the circuit was interconnected as in Figure 29 and plugged to the spark plug for its testing. First of all it was tested at atmospheric pressure and as it successfully generated the first sparks was brought into the vacuum chamber.

The first set of tests were carried out at a pressure of 4E-5 Torr, leaving the circuitry outside the vacuum chamber for easier accessibility. Furthermore, other reason for that was that at this point of the experiments the vacuum chamber was taking about 5 hours to reach such pressure and resulted extremely impractical to stop it to manipulate the circuit.

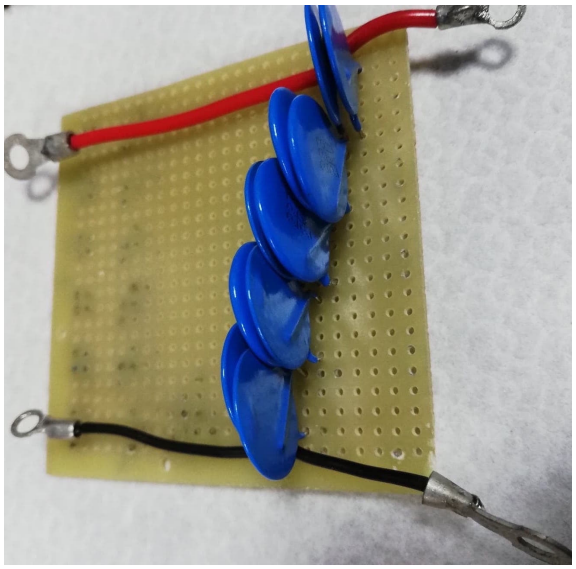

Figure 28: Capacitor bank sub-circuit

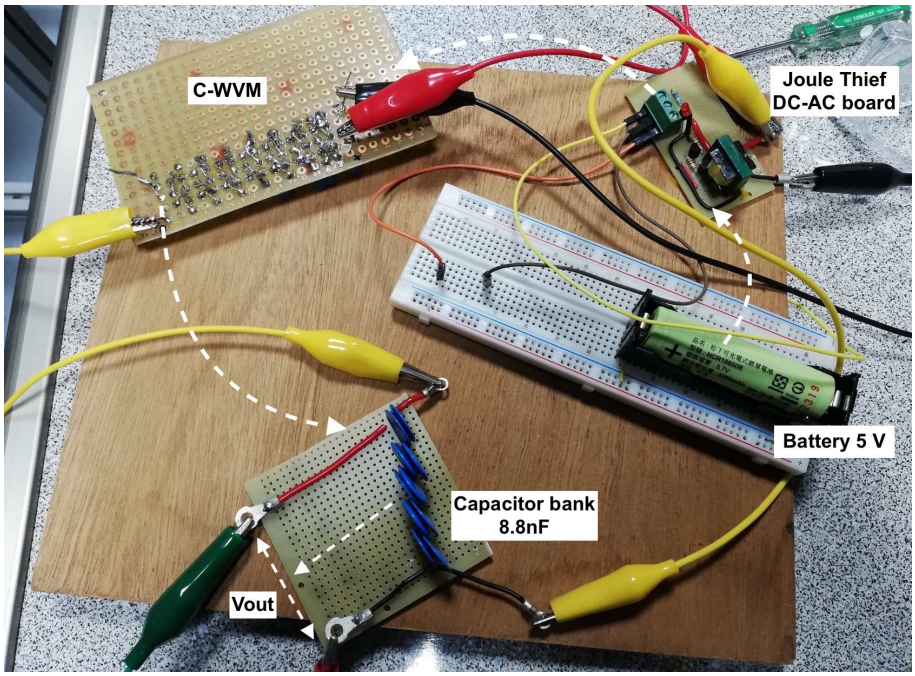

Figure 29: Complete assemble of the testing breadboards circuit

The breakdown was reached and several sparks were visible on the sparkplug terminals. Although it produced the first controlled sparks, it did not last long due it just produced a few discharges before suddenly stopped working. During the next days the voltage multiplier was examined without any finding of apparent reason for failure. The voltage measured at its output reached a maximum of 5 kV.

After some days of research and testing, a malfunction in one diode was found

in the 6th stage. The faulty diode presented a leak that apparently was the reason for the odd behavior in the voltage multiplier. Although the reason for its failure was unknown, it was replaced and tested again. The circuit generated 8 kV and the breakdown in vacuum by the sparkplug was possible one more time. Hence, was proceeded to integrate the main discharge circuit altogether with the sparkplug.

After working in the ZAP lab of NCKU for slightly more than 1 month, the first successful discharge was achieved.

Figure 30: First PPT discharge at a pressure of 3E-5Torr

Pressure	3E-5 Torr
Pulse length	100 ms
Discharge energy	3.6 Joules
Discharge freq.	7 sec

Table 4: Parameters for the first successful discharge in vacuum

Test 2

Although the first set of discharges were obtained, the performance of the circuit was not the expected and rapidly it started to decay. After few hundred of tests, it continuously delivered 6 kV which in principle was enough to reach the breakdown voltage in the sparkplug, but it clearly showed a constant problem on the circuitry manufacture.

Therefore a research was carried out and in search for answers and after few days was found in [24][27] that as the C-WVM is a voltage multiplier, the current is getting disminished at every stage because the impedance of the capacitors and

the resistance of the diodes, influencing directly the voltage drop at the oputput. In [26] was observed how in voltage multipliers over 7 stages, the performance gets affected because the very low current, thus an optimization of the voltage multiplier was needed.

Different configurations have been analyzed in [27] where among others, the ladder-decreasing capacitance is commonly used [28]. It consist of having a higher capacitance at the lower stages (considering the input as the lower level) and gradually decrease their value in the following stages. This configuration has as purpose to provide a higher current to furthermore stages. The capacitance arrangement follows the reason:

$$C_{array} = C_N \cdot N, C_{N-1} \cdot N_{-1}, C_{N-2} \cdot N_{-2} ... C1, \tag{14}$$

where C is the base capacitance located in the last stage and N the total number of stages.

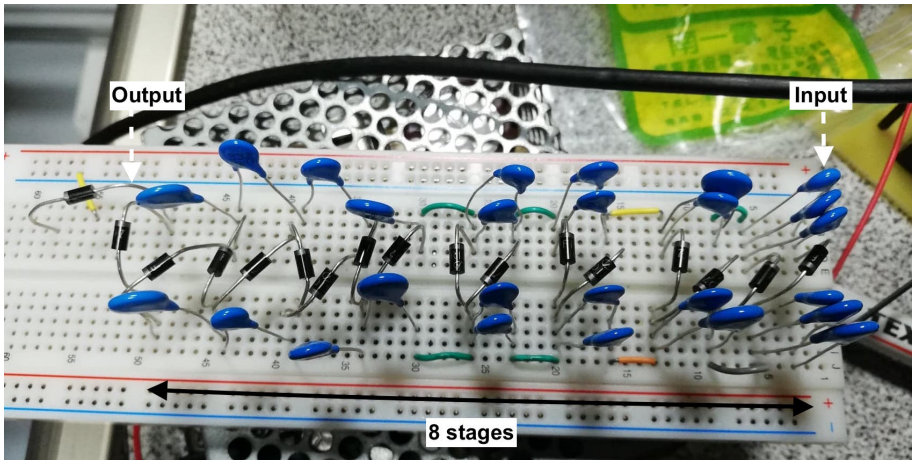

Figure 31: CWVM with a ladder- capacitance configuration using 8 stages

After implementing this configuration the voltage at the output rose again to 8 kV allowing a longer set of experiments. The first set of tests, corresponded to a sequence of experiments by an other student from the ZAP Lab, whose research was directed to test a set of nozzles for plasma expansion on PPTs. Although it is not relevant for this research, the circuit was testes for around 150 discharges using different range of energies in the main discharge circuit (from 2.8 J to 4.5 J), and a range in between 50 ms to 100 ms for the discharge time of the sparkplug , showing an inconsistent discharging rate, with a high rate of missfires of about 40%.

This time the reason was attributed to the mechanical sparkplug and the set of nozzles. Hence, these were removed and the anode of the sparkplug was changed for an enhanced version. Once the experiments were retaken and an improvement was clearly observed. After 250 shoots having 100% of successful discharges.

It allowed to set longer tests, leading a series of experiments proving hundreds of unsupervised fires. The circuit was set into the vacuum chamber and thanks to a student from the Zap Lab who developed a software to count the number of discharges using a web cam and image recognition, was possible to get a closer view of the long run behavior of the system.

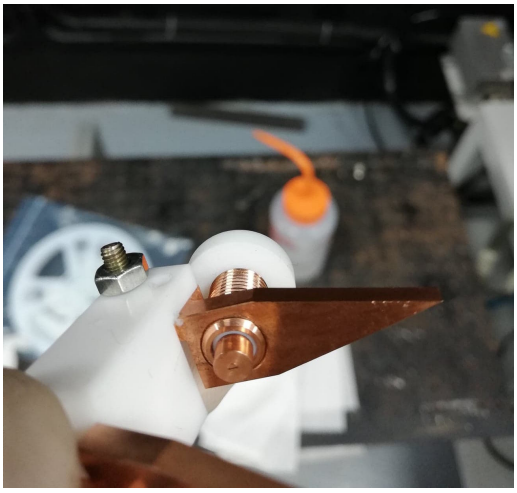

(a)

(b)

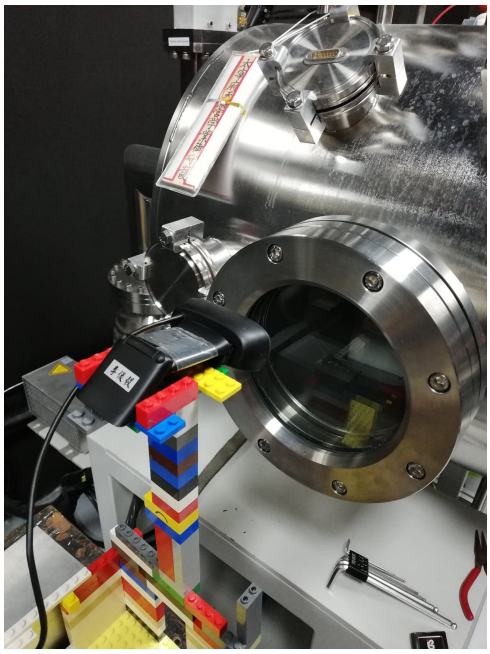

(c)

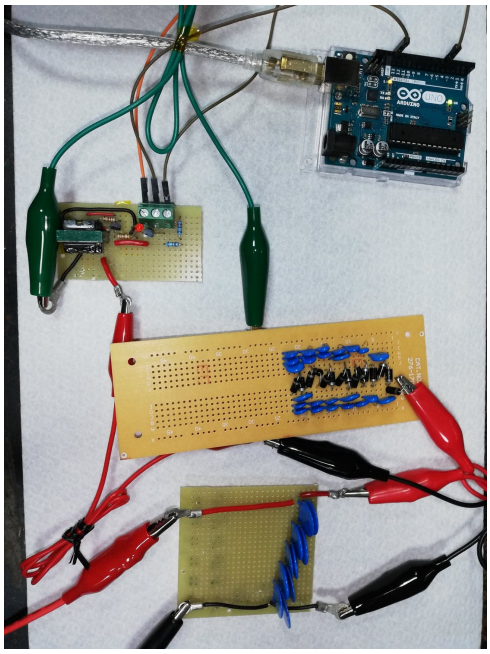

(d)

Figure 32: a)and b)Enhanced sparkplug. c)Web cam used to count the discharges. d)Complete circuit used for the long run tests with the C-WVM soldered on a new breadboard

The results obtained were not satisfactory as expected due the circuit stopped working for problems with the MCU after few thousands shots, according to the records. Nonetheless, a 100% of successful discharges was achieved.

During the following days after the experiment, few test were carried out but a constant problem on the diodes was faced. Apparently they continued failing for an unknown reason and the board had to be fixed several times.

Without clear reason of this issue, it was decided to consult an external engineer who could gives a proper guidance to identify the problem.

As a result, the odd behavior was related to the reverse voltage of the diodes used and the input voltage on the voltage multiplier. There is not enough information available about this topic, but according to [29] there is a relationship between the peak input voltage V_p and the reverse voltage in each diode, being:

$$V_{diode} = 2V_p. \tag{15}$$

When the value $2V_p$ is close to V_{diode}, a small current called leakage current flows through the device, otherwise when this voltage exceeds the limit, the device may fail. This relationship, and in concordance with the Equation 15, helped to analyze the loop from a different perspective and cleared the previous theories. It also pointed out the necessity of using diodes rated at 4 kV reverse voltage, which is non-viable because there are no diodes rated at that voltage and making arrays in series only would result in a bulkier system

Following the aforementioned, the experiment was stopped. The Joule thief limitation was understandable for a product that was recycled from other circuit and thereby it did not allow its full control. Even though it worked as a baseline to understand the behavior of the C-WVM. With this vision the project moved forward and the efforts were now focused into the design of a circuit able to fulfill the new requirements.

4.4 High voltage Fly-back converter and Cockcroft-Walton Voltage Multiplier

After the valuable lessons learned while working with the C-WVM it was decided to continue in this direction. Nevertheless, due its functionality principle of working with AC the need to considerable space to display all the necessary stages, it result impossible to achieve the goal of 8 kV as an output. Therefore a high gain pre-step up stage was required. At the same time this configuration should act as a interface between the logic and the power sections. In summary, the main features needed for a topology were:

Input Voltage	5-8V DC
Output Voltage	$V_o \leq 1000 V_{p-p}$ AC
V_o regulation	Software
Isolation	Galvanic
V_o frequency	in order of kHz
Dimensions	40x30x20 mm
Output Power	2.25 Watts
Power consumption	2-3 Watts

Table 5: Requirements for a pre-step up stage

Consequently, once have been careful considering and taking into account the different advantages and disadvantages that different configurations offer such as low power, simplicity, isolation and cost, the flyback configuration was chosen[20][32][35][34].

The concept of flyback converters can be described as two loops with or without contact in between them, affecting each other through a magnetic field generated by one of them. This effect is known as magnetic couple [31]. Transformers and coupled inductances are devices that take advantage of this principle by using magnetically couple coils to transfer energy from one circuit to another without a physical wired connection. Moreover, it is said that when two coil are close each other and a change in the current of one coil affects the current and voltage of the second coil, the changed can be quantified by a property called mutual inductance.

There are different kinds of coupling being the most common air, iron and ferrite. The last ones are of special interest due the ferrite core are typically used in radio-frequency applications because it good properties working at high frequencies and it is well known that high commutation frequencies help reducing armonic distortions. A typical figure for efficiency in a fly-back circuits is around 65% to 75%. [35] in low voltage applications and 80 to 85 for high voltage applications.

Looking at the Figure 33 the functionality of the Flyback converter can be summarized as:

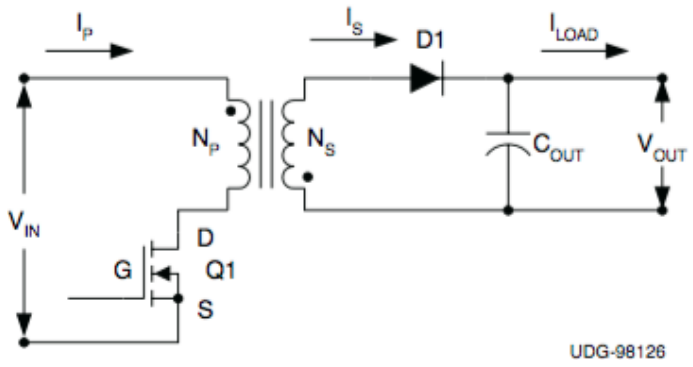

Figure 33: Typical Fly-back topology [33].

- When the switch is closed in a time t_{on} the inductance denoted as N_p storage energy from the the power source, while the load at V_{out} is supplied by the C_{out}
- When the switch is opened in a time t_{off} , the capacitor and the load or V_{out} are now supplied by the second inductance N_s .

Nevertheless, the traditional Fly-back is meant to operate as a DC-DC step up converter, whereas in the requirements has been remarked the need of an AC output. For this reason a different approach has been taken in consideration where the diode D1 and thee C_{out} have been removed. In this way the output waveform is a semi-sinusoidal wave product of the commutation of the transistor Q1. The resulted circuit can be then re-drawn as:

After haven redefined the circuit specifications, the next step is to determine the duty ratio, which is a crucial factor for it design and operation. It has to be taken in consideration that according the application, Flybacks have two types of operation modes: continuous conduction mode (CCM) and discontinuous conduction mode (DCM). The difference between each other lies in the behaviour of the current. While in CCM the current never goes down to zero, in DCM it does.

The election between the distinct modes is usually determined by the application. For high output voltage and low current applications DCM is typically preferred because it provides better switching conditions when the rectifier is used, since the diodes are operation at zero current just before being reversed biased. The couple inductances size can be reduced, because the average energy storage is lower than if CCM is used. Nevertheless, DCM causes high RMS currents in primary and secondary RMS up to two times higher for discontinuous mode than for CCM leading to DCM to require a transistor with a higher current rating.

On the other hand, CCM is preferred for low voltage and high current output applications. This also facilitate the design process since the input to output voltage gain depends directly on the duty cycle. However it has the disadvantage of requiring a higher magnetizing inductance to stay in CCM the entire operating time range and a right-half-plane zero in its transfer function[33][36].

Even when Flyback converters are relatively simple, they need to go under a detailed design process where some important factors have to be taken into account at the moment of design.

Switch selection

In power electronics the use of high frequency switches is widely used and the most common are the IGBT and MOSFETs. The working principle description is out of the scope of this manuscript but, the use of a MOSFET is proposed. The main reason lies on the saturation voltage for IGBT typically is higher than the logic voltage of the microcontroller and it would imply the addition of an extra circuit to step up the logic voltage from the MCU . Nonetheless, among the wide selection of MOSFETs, there is a logic-gate variation which can be saturated from 3.6 to 7 V, allowing the full control directly by software.

This led to review some considerations before to choose any component, as is the power that it is able to dissipate. This relation is given, first off all for its estimated efficiency where:

$$P_{in} = \frac{P_o}{E_{ff}}, \tag{16}$$

as the efficiency for high voltages is around 80% and the P_o is estimated as 2.5 Watts it results in P_{in}= 3.3 Watts. This means that at $5V_{in}$ the input current I_{in} is about 600 mA. In the case that the DMC is planned to be used, the worst scenario has to be calculated. This is the RMS peak current coming back to the transistor and it can be estimated around 850 mA, meaning that the MOSFET dissipation power has to be at least 1 A.

In the same way, the working frequency at which the MOSFET has to be switched is determined by the MCU. For this particular case the as higher frequencies are desired, the maximum frequency at which the flyback aims is 62.5 kHz as is described in more detail in chapter 5. Leading a switching time of at least 16 μsec.

Finally the MOSFET chosen was the IRL530n whit characteristics:

Saturation voltage	4-7V DC
Source-gate Voltage	100 V
Source-gate current	17 A
Commutation speed	MHz
$\mathbf{R}_{DS}$	0.10 Ω
Operation temperature	−55 to +175C

Table 6: IRL530n logic-gate MOSFET

As it can be appreciated in the Table 6 all the factors aforementioned are under the limits of the MOSFET and due its logic-gate voltage and low cost, it resulted suitable for the application. Additionally, the use of DCM is completely safe and therefore it will be used.

Duty Cycle

The first step before to calculate the duty cycle is to determine the rate of turns our coupled inductance needs. In an ideal FB, together with the duty cycle the turns rate is directly proportional to the output voltage

$$V_o = \frac{N \cdot D}{1 - D} V_{in}. \tag{17}$$

This equation is the product of the derivation of the flyback's transfer function, where N is the turns ratio in between the inductances and the gain the of the circuit. This can determined by

$$N = \frac{V_o}{V_i}. \tag{18}$$

Now, considering the requirements stated in Table 5 a gain N= 200 is needed. In base of that, is just matter to substitute the Equation 17 to get a theoretical duty cycle of 50%.

Contrary what can be consider, where every time the duty cycle D increases towards the unity or 100% but without reach it, the voltage V_o tends to increase but in reality this is not what happens. The reason is because in the equations, losses associated to parasitic elements and heating are not considered [37]. Moreover if the principle of PWM is taken, the higher the duty cycle on the MOSFET reflects the longer the time this will be conducting until reach the 100% what means being in ON state the entire cycle.
In other words, the primary inductor will be conducting or "charging" during all the cycle and it will never be able to generate the magnetic field associated with the change in the current flow reflected in the secondary inductor, meaning a poor or null gain.

Is important to note that the results obtained from this formula are close to the reality but there always exist small leakage currents product of a physical coupling factor that can only be determined from direct measurements to the device.

Having been this calculated, a simulation was carried out to determine the functionality of the envisioned array together with the voltage multiplier. This can be seen in the Figure 34:

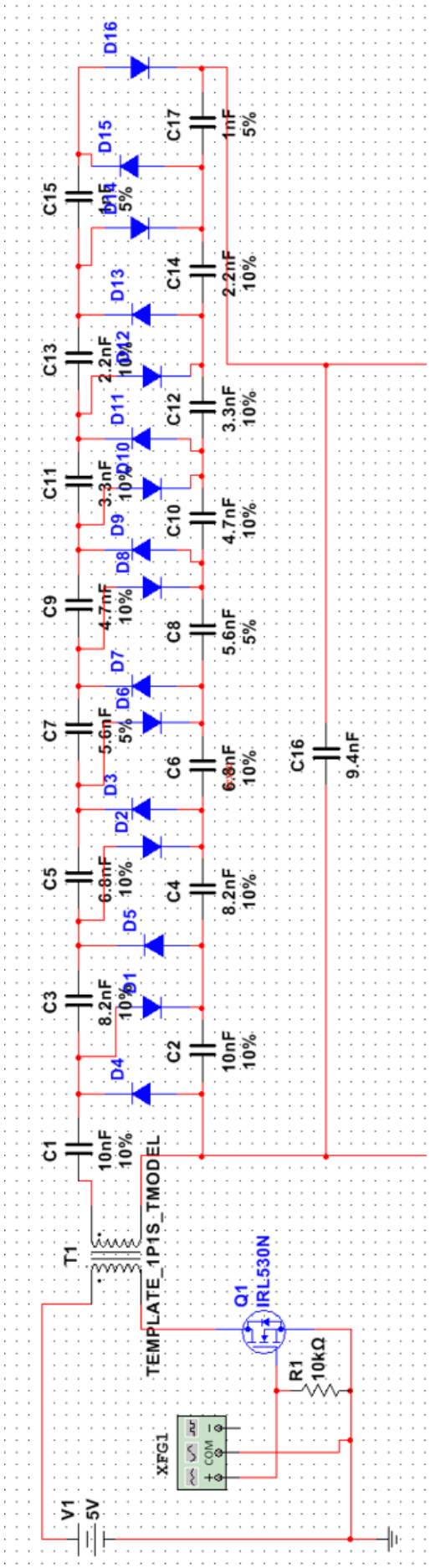

Figure 34: Fly-back and C-WVM.

Testing and validation

After have gotten successful results during the simulations, the prototyping was carried out. The coupled inductance was purchased to Shaanxi Full-Star Electronics, a regional company whose dedicate to the manufacture of inductors and transformers for high voltage. Although the size was not as compact as desired, the cost-benefit seemed very attractive due they offered an semi-custom made inductance guarantying a high performance. The detailed information about it can be seen in more detail in the Appendix of this thesis.

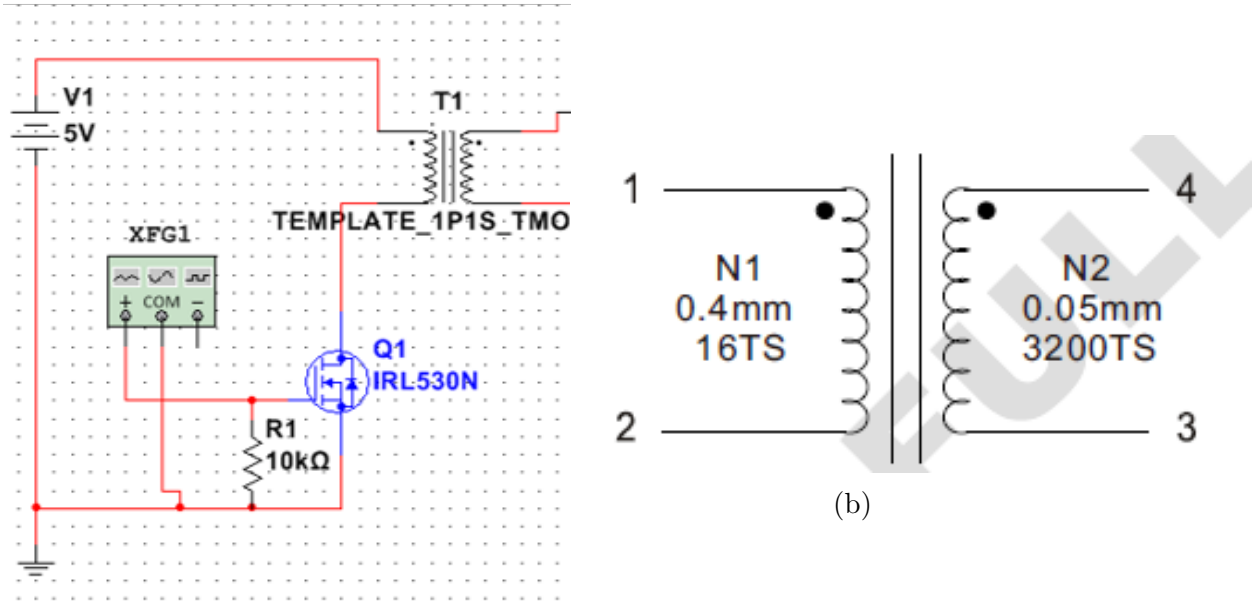

(a) (b)

Figure 35: Coupled inductance by Full-Star with N=200

In Figure 35 is pictured the schematic of the inductance showing the turns ratio in between them and the wire width used in each coil.
Moreover, the aforementioned coupled inductance meet the following characteristics according with the manufacturer:

- Compact size
- 1-200 turns ratio
- Inductance (2-1): 22-29 μH
- Inductance (3-4): 470-570 μH
- Input 5 V – 24 V
- Output 1 kV – 4.8 kV

The circuit was mounted into a protoboard as is showed in the Figure 36a, and this was commanded by the MCU using a variable duty cycle of from 40 to 75%, resulting the 60% the best option as demonstrated by the equations. This decision was taken considering the higher voltage obtained and the heat dissipated by the FET.

The circuit continued being tested for a couple of days to observe its behaviour, and once it seemed reliable enough the first long-run test was prepared.

The test was done by the student from the ZAP Lab who was working on experimental designs for different electrodes shapes with the purpose to increase the exhaust velocity of the charges particles in the plasma. As the test was planned to run overnight, was used the previous developed software to count the number of discharges. The set-up of his discharge counter worked god enough to give an estimation of the behaviour of the circuit and the thruster.

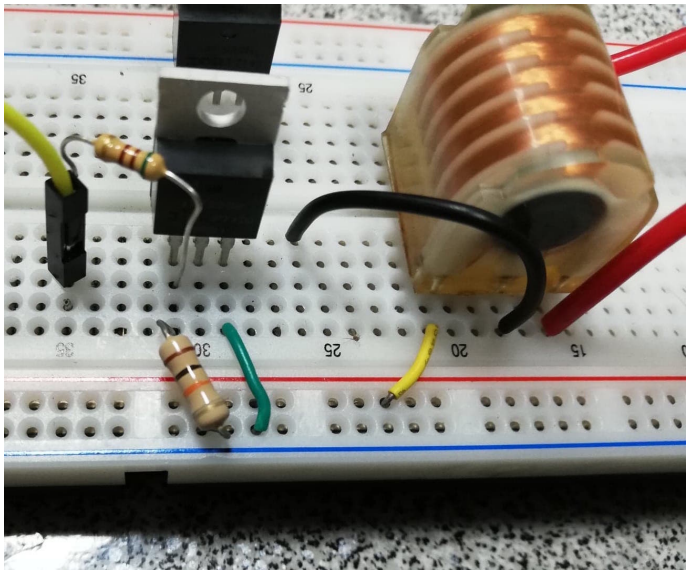

(a)

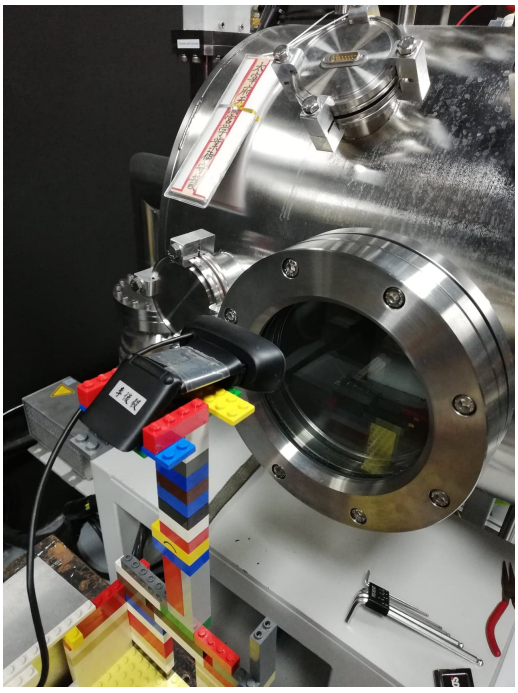

(b)

Figure 36: a) Flyback setup for the first long-run attempt. b) Discharge counter setup using a webcam and image recognition software.

After 17 hours of test the results were the following:

Pressure	5E-7 Torr
PWM frequency	32kHz
Duty cycle	60%
Pulse train length	100ms
Input voltage	5 volts
Operational voltage MDC	1500 V
Operational voltage SPC	7-8 kV
Frequency of discharge	7 sec
Test length	17 hours
Total discharges	7500
Success rate	85%

Table 7: 1st long-run test campaign results

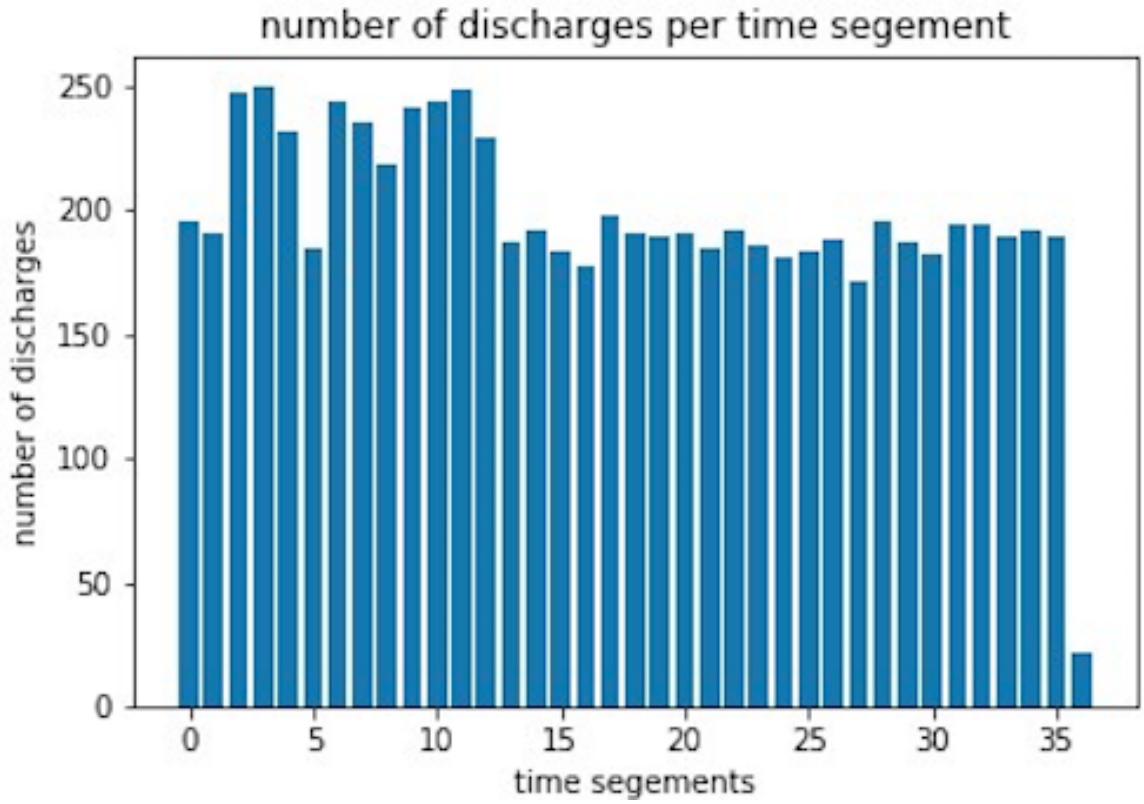

Figure 37: First long-run test campaign results.

In Figure 37 was plotted the approximated results in segments of 30 minutes. Although the software seemed to work fine, a slightly higher successful rate could be considered due the counter program was in its first version and therefore cannot be taken as 100% reliable.

5 Microcontroller Unit (MCU)

Pulsed plasma thrusters are said to be one of the simplest electric propulsion systems. This concept lies on the main idea of how do they work by inducing controlled pulses in a periodic fashion. Hence, the use of a microcontroller was essential and during the current chapter will be described the implications that it brings with it.

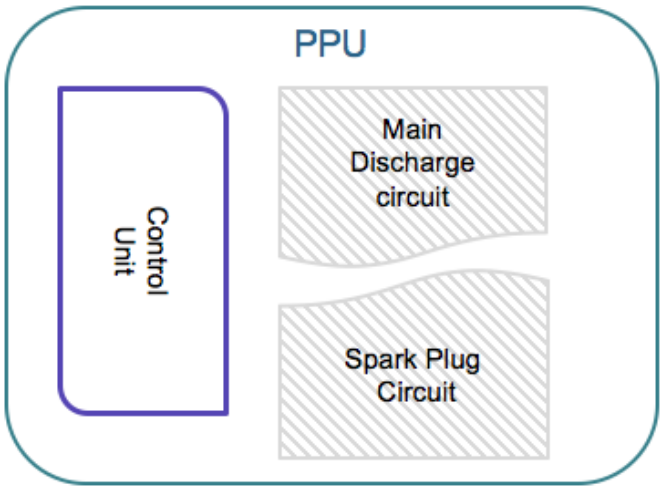

Figure 38: PPU: Microcontroller Unit

5.1 Early analysis

A microcontroller is an integrated circuit (IC) capable to execute commands pre-programmed in its memory. It usually contains a CPU interconnected with a series of memory devices, PIUs, timers/counters, etc. These devices have the capability to take inputs from sensors and directly control actuators, making it suitable for the current purposes.

In order to fulfill the requirements of the system, some basic considerations had to be taken as are:

Once established the aforementioned requirements, a suitable and fast solution was the well known Arduino Uno platform. Its features as open source platform and to be a "Commercial Off-the-Shelf" (COTS) device, made it a good choice to look into it. Therefore, it will be analyzed for its implementation in this project.

Clock Freq.	The system itself does not require high operation frequencies, but 100 kHz is desired
GP Outputs	An estimated 5 outputs minimum to control the sparkplug and the main discharge circuit DC/HVDC converters.
Duty cycle	60%
PWM	4 Ports available with at least 8 bits resolution.
Communication protocols.	The MCU has to support communication I^2C and/or UART
Operational voltage	3.6- 5 V
Response degree of the system.	*Firm Real Time System* can be considered as an acceptable response for the targeted application[39]
Extra	Low cost is a plus

As was mentioned before, Arduino Uno is an open source platform board based on the use of an Atmega328P as microcontroller. This brings up the versatility and availability of resources, speeding up the development of the subsystem. It has 14 I/O digital ports (which 6 can be used as PWM outputs), 6 analogue inputs, 16 MHz crystal oscillator, USB connection, power Jack and as a serial driver chip it features the Atmega8U2 programmed as a USB-to-serial converter for an easiest uploading the code from the Arduino IDE, which is supported by Windows, Mac OS and Linux.

Technical specifications

Microcontroller	Atmega328p
Operating Voltage	5 V
Input voltage	6-20 V
Digital I/O	14 ports
Analog Inputs	6 ports
Clock Frequency	16 MHz
PWM ports	6 ports up to 31 kHz
Flash memory	32 KB
EEPROM	1 KB
Communication protocols	I^2C, UART, SPI
Cost	20 €

Table 8: Arduino UNO technical specifications

Even when its internal clock runs at 16 MHz, the PWM is not running at the same frequency. This happens because the PWM ports are ruled by 3 different timers: timer0, timer1 and timer2. Timer0 and timer2 are 8 bits resolution while timer1 has 16 bits resolution, limiting its maximum frequency to 31 kHz and 62.5 kHz respectively, which in principle is enough for the application[41] .

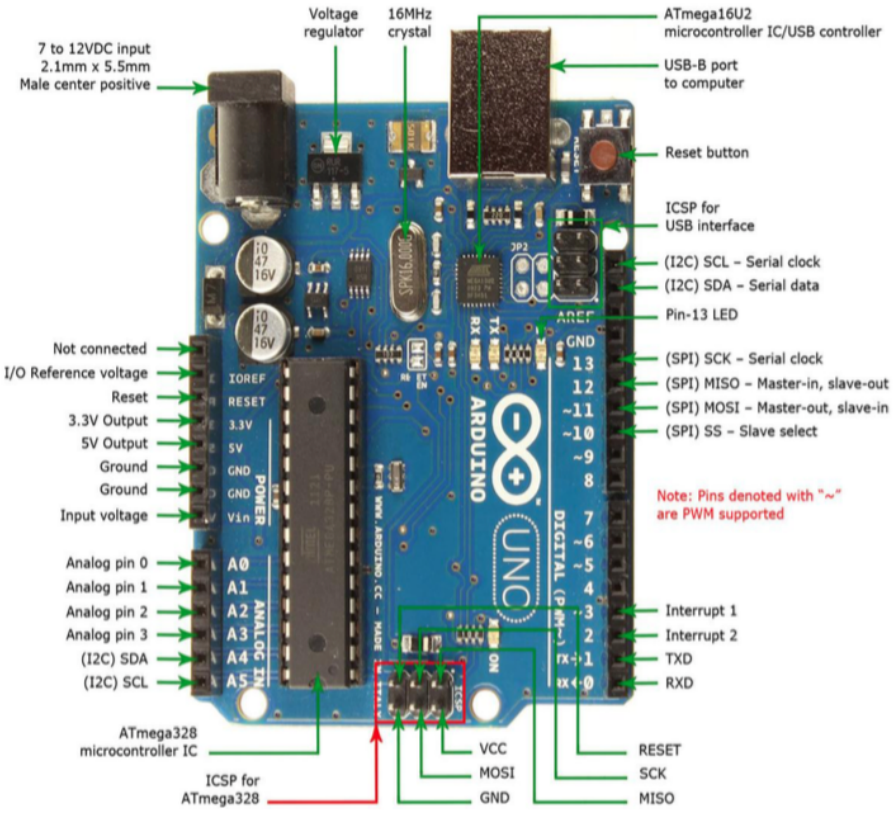

Figure 39: Arduino Uno pin out[40]

6 Experimental results

After have been testing the circuits and have gotten a descent rate of successful tests (90% out of 11,000 discharges), the project moved forward into manufacturing the PCBs for the sparkplug and main discharge circuit. Furthermore, a new set of the electrodes and the mechanical enclosure were designed by the team of mechanical engineers of Odysseus.

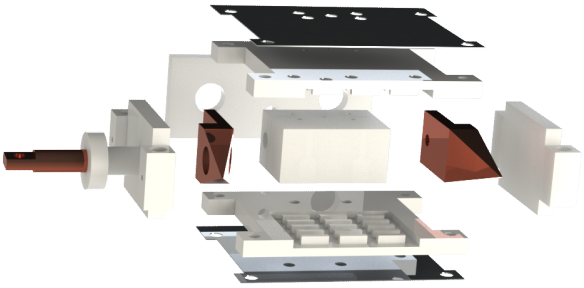

(a)

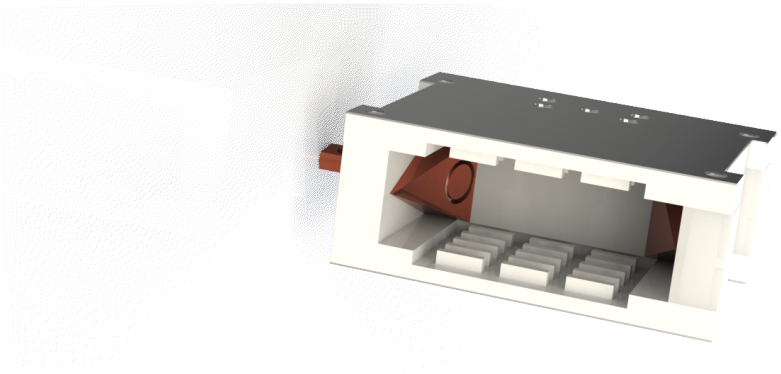

(b)

Figure 40: Renders of the full PPT body assemble developed by Odysseus Space Inc. a) Exploded view of the electrodes in its enclosure b) Assembled box for one thruster.

Although the project management had stipulated test of the final prototypes during the last month of work, the schedule was shifted a couple weeks due some unexpected delays from the machining manufacturer, which led to rush a set of experiments at the last 2 weeks of this work. During this time, the SPC was manufactured and delivered for the first set of tests. The circuit was plugged to the previous sparkplug and controlled by the breadboard control circuit.

Test 1

As aforementioned, the first tests for the final prototypes started with the SPC. The goal was to proof its behaviour using surface mounting components instead the typical through the hole used in the breadboards. The main concern was the creepage in between the components as it was not manufactured with any special

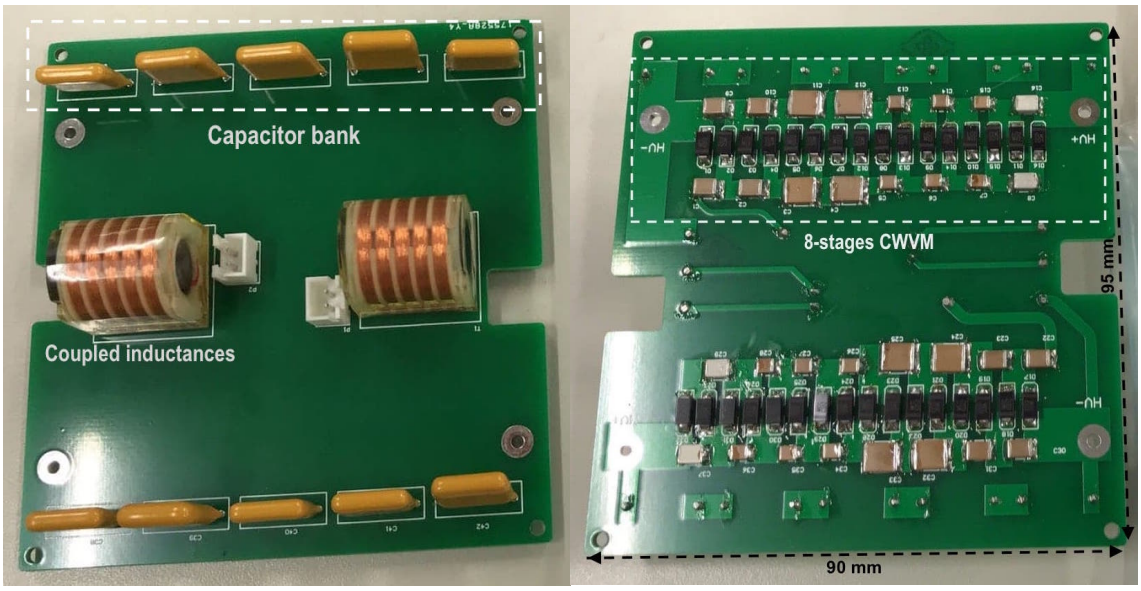

(a) (b)

Figure 41: Final PCB prototype for the spark plug.

pottering for high voltage.

The first test was run with the circuit plugged to the current set of electrodes and these were placed inside the vacuum chamber, leaving the PCB outside for its easier manipulation. The conditions of the experiment were:

Pressure	5E-7 Torr
PWM frequency	31 kHz
Duty cycle	60%
Pulse train length	100 ms
Input voltage	5 volts
Frequency of discharge	5 sec

Table 9: Test parameters for spark plug circuit

After the first attempt, no sparks were observed either in the spark plug and on the circuit. Thereby the first idea was to increase the length of the pulse train from 100 ms to 150 ms still without any signs of corona discharge. Hence a periodic increase of the pulse train length was performed in increments of 50 ms until reach 350 ms. At this point was visualized the first sparks, although it behavior was not consistence.

In this way the test was paused to instead measure the output voltage of the circuit with the oscilloscope and its latency. To do this the HV probe was connected directly to the output terminals of the circuit and the length of the pulse train was

increased in order to observe the time it takes to reach its peak voltage.

However, once this was done a thunderous spark was generated on the surface of the board after the voltage overcame 8 kV. After this happened, the components were inspected one by one with the help of a multimeter and a capacitance meter, resulting damaged a couple of diodes and completely inhibiting the circuit. This led to stop the experiments in atmosphere an sent the circuit back to the manufacturer for the replacement of the damaged diodes.

Test 2

This time the experiment on the breadboard circuit was retaken and the new set of spark plug and electrodes recently manufactured. A quick test was run of about 15 min, with a discharge frequency of 5 seconds, resulting in ∼180 discharges from which 90% of them were successful. However, this 10% of failure apparently was not coming directly from the SPC itself, but from the mechanical SP. This conclusion comes from the observation at the moment of the operation where was noticed a constant but dimmed and *yellowish* spark instead of the *bluish*/white that induce the breakdown of the circuit. The reasons of these phenomena are still unclear but earlier theories suggest the carbon coating formation observed in Figure 42 b) and c) was the reason of the apparent short circuit. It resulted atypical due the formation of the carbon film usually appears after some hundred discharges and get consume after a couple of misfires.

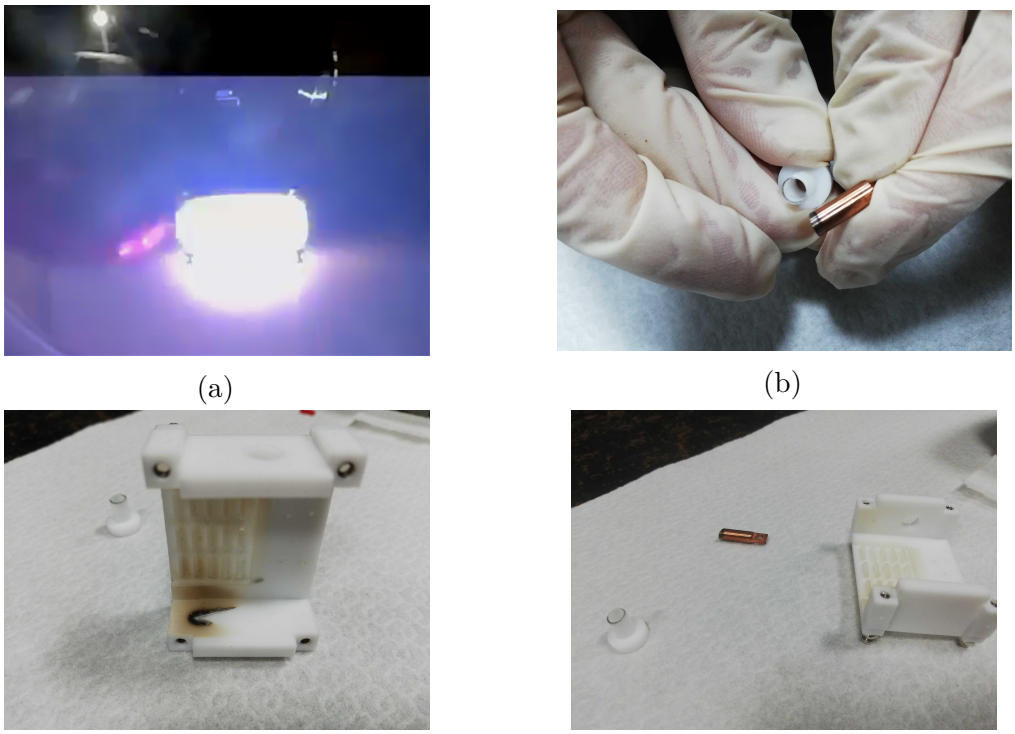

(a) (b)

(c) (d)

Figure 42: a) PPT discharge b) Carbon coating on the SP anode and on the PTFE insulator. c) Anode-side wall of the box covered by a carbon coating by the ignitions. d) Opened view of the cathode-side of the PPT's box.

Test 3

The breadboard circuit was repaired and the tests were retaken. Now, with the purpose to avoid flash overs, the circuit was placed into the vacuum chamber next to the PPT. The carbon coating was sanded down and the anode was replaced for one slightly thinner and covered with Kapton tape to avoid surface flashover through the PTFE. The idea was to ensure the ignition through the gap in between the anode and the cathode of the spark plug. This worked well for 35 minutes (∼420 discharges) having a 98% of successful ignitions before it completely stopped working.

Consequently, some hypothesis were formulated on what is leading the strange behavior and limiting the ignitions to a few hundred. After the brainstorming, some actions were performed as they were:

- SPC was tested separately from the SP electrodes to observe if it has been damaged or presented any malfunction. It resulted working normally and no unusual behaviors were noticed.
- The SP was connected to the circuit and tested in atmosphere conditions only with the intention to discard any wiring problem in between. See Figure 43a.

- The circuit was integrated back again and the vacuum was induced. The circuit worked for another 5 minutes and then stopped once more again. See Figure 43b.

This experiments clearly showed an odd behavior after few discharges, while the circuit seems to be working normally there is not ignition on the spark plug. The reasons were unclear, but everything pointed to a mechanical issue and possible short circuit due carbon coating in between the electrodes preventing them to reach the breakdown voltage and consequently the spark.

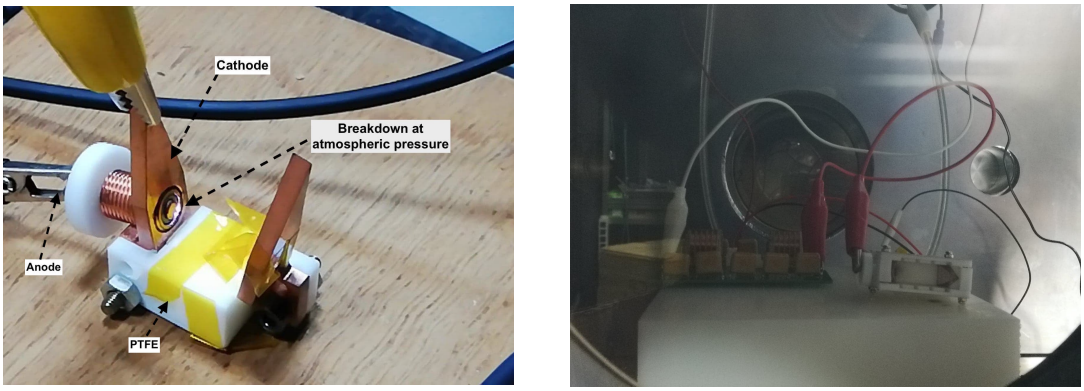

(a) (b)

Figure 43: a) PPT discharge in atmosphere b) SPC next to the PPT inside the vacuum chamber.

Test 4

Since the test campaign started, was noticed the necessity to increase the length of the pulse train needed to reach the spark in comparison with the breadboard model. While before typically used 70-100 ms per fire, now the circuit was needing 100-200 ms to perform the breakdown. This behaviour seemed to have no good reason to be, except for the individual components. The capacitors used for the PCB were slightly different than the ones used in the design campaign, allegedly of superior quality. So, for the sake of discard any discrepancy on the components, the capacitor bank was first disconnected from the PCB as is seen in Figure 44a and the voltage multiplier was tested, resulting in a similar behaviour than its predecessor version.

Therefore, it can only mean something: the capacitor bank was causing an undesired delay at the moment of charging/discharging and consequently it was replaced using the previous components. See Figure 44b

After have replaced the capacitors, the SP was sanded down, cleaned and a long test was scheduled in to be run during the weekend. The goal of the test was to proof the reliability of the new capacitors and the SPC itself for the long term. The data collected by the test is displayed in Table 10.

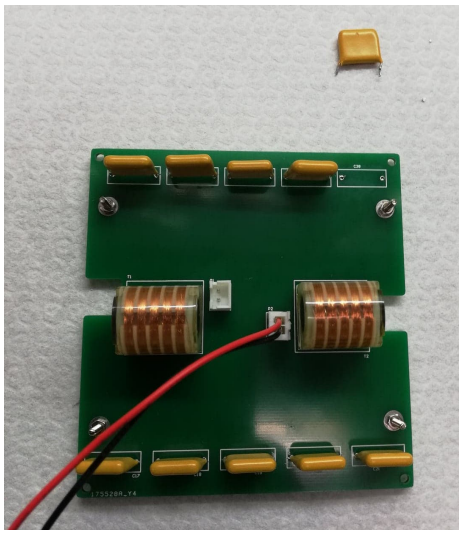

(a)

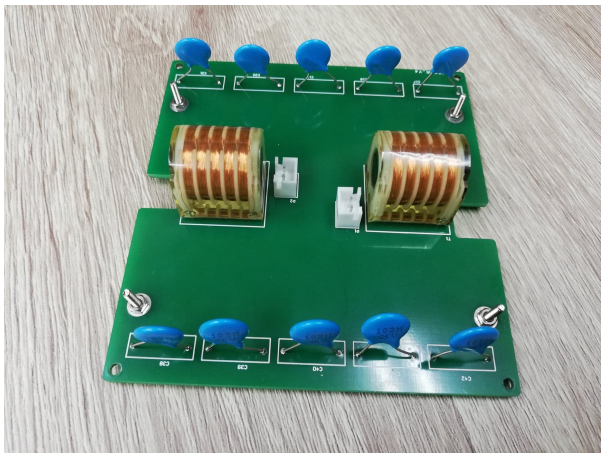

(b)

Figure 44: a)Capacitor bank disconnected from the SPC b)SPC after have replaced the capacitor bank.

Pressure	5E-7 Torr
PWM frequency	31 kHz
Duty cycle	60%
Pulse train length	100 ms
Input voltage	5 volts
Operational voltage MDC	1500 V
Operational voltage SPC	7-8 kV
Frequency of discharge	7 sec
Test length	20 hours
Total discharges	7500
Success rate	75%

Table 10: 2nd long-run test campaign after have replaced the capacitor bank

It has to be said, that the data was produced by the software developed by other student of the ZAP Lab, who by the date of the tests was not more in the lab and the software seemed to miss several fires, meaning that from the 75% calculated, it could have gone up to 90% according with the observations during the first 3 hours, where all the discharges were successful. Nevertheless, according to the registers, where not even one fire was registered, the circuit stopped working at for the last hour.

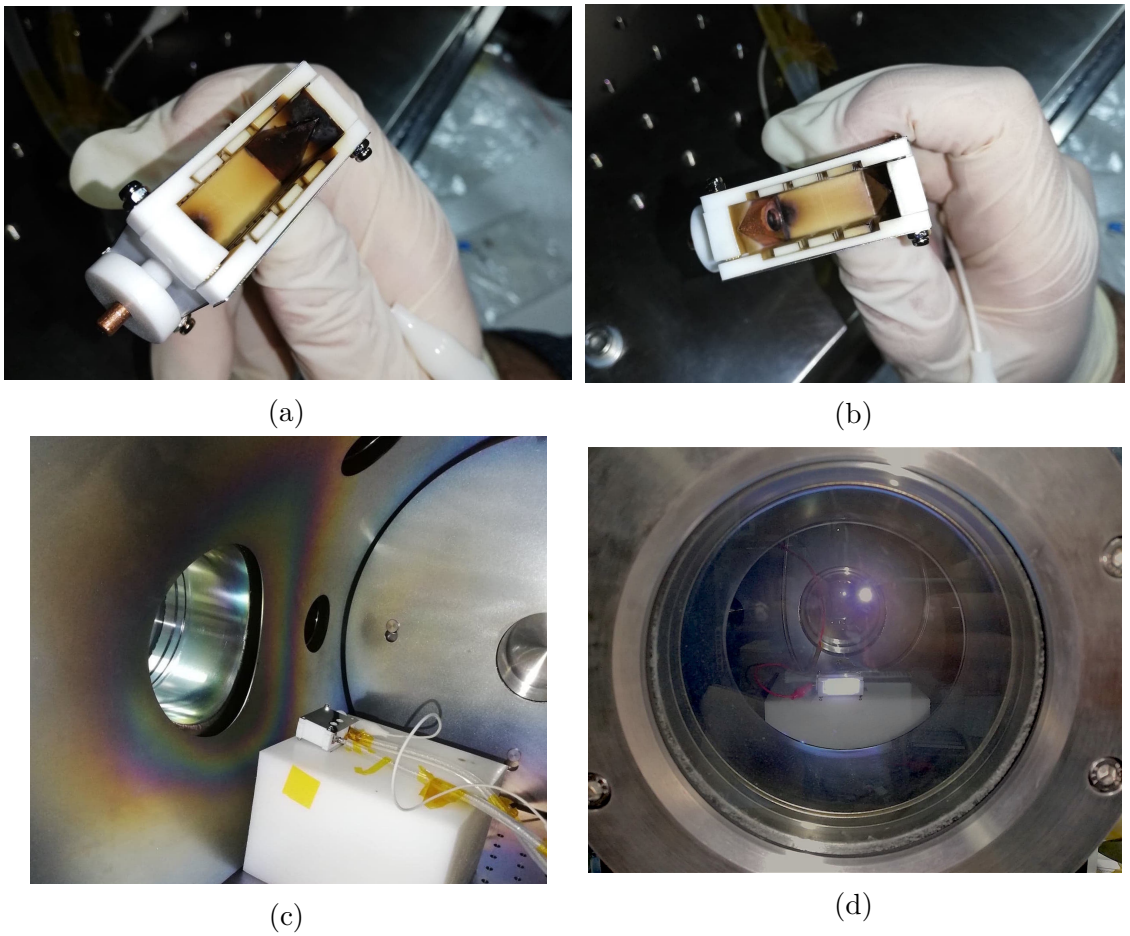

(a) (b)

(c) (d)

Figure 45: 2nd long-run test a)PPT's anode cover by a considerable layer of carbon, specially at the tip of it. b) PPT's cathode cover by a light layer of carbon c) Rainbow effect caused by the plasma. d) PPT being fired in the vacuum chamber at a pressure of 3E-7 Torr.

Moreover, as extra observation can be appreciated in Figure 45a and 45b how an extensive carbon coating film is accumulated at the end of the anode of the PPT. As this was the first long run test carried out. From the Figure 45c can be seen how the rainbow effect spotted in [17] left a big mark on the hatch from the vacuum chamber.

Test 5

Along this work, has been broadly talked about the impact of the carbon formation on the SP and how it affects the performance of the system without really tackle the problem directly. It is largely due the tight schedule for the project itself, making not impossible but challenging the development of the entire PPU. However, although these last test were carried out in the last weeks of the research, a new idea came out. During this last campaign of test, is presented the introduction of a *Spark gap* which as its name state it, is no more than a gap in between the SPC and the SP electrodes. See Figure 46

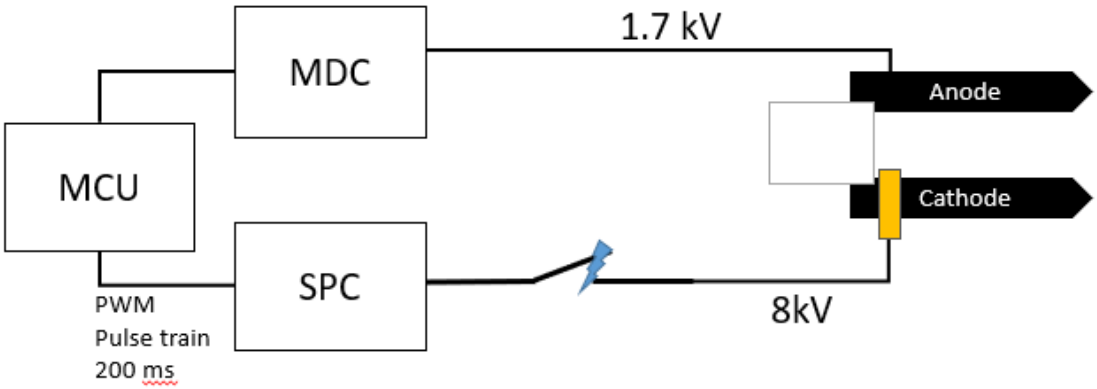

(a)

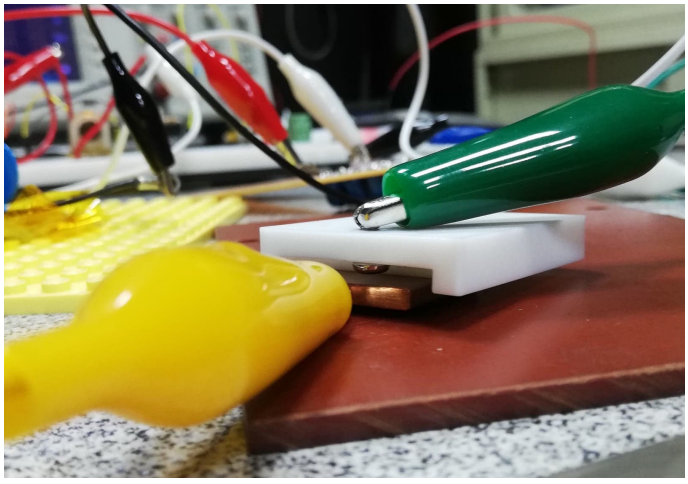

(b)

Figure 46: Spark gap implemented to ensure the capacitor bank reached 8 kV

The idea behind this gap is to force the SPC to reach 8 kV regardless if the electrodes were short circuiting due the carbon print. Although the implementation was a bit sketchy, it served as proof of concept where an air gap acts as a barrier between the two plates and only being overcome when the breakdown voltage is reached.

Fortunately the MDC PCB arrived in the last moment of the project, giving a very short but enough margin for testing and provide the evidence of functionality that validated 5 months of work. See Figure 48. Thereby the integration of the different subsystems was carried out and the test were settled under the same conditions as previous campaigns (see Table 11) except for the fire frequency, which was now speed it up to 0.2 Hz. Figure 47

Pressure	5E-7 Torr
PWM frequency	31 kHz
Duty cycle	60%
Pulse train length	100ms
Input voltage	5 volts
Operational voltage MDC	1600 VDC
Operational voltage SPC	7-8 kV DC
Frequency of discharge	5 sec
Test length	60 hours
Total discharges	40000
Success rate	92%

Table 11: Final test campaign with all the SPC and MDC PCB integrated.

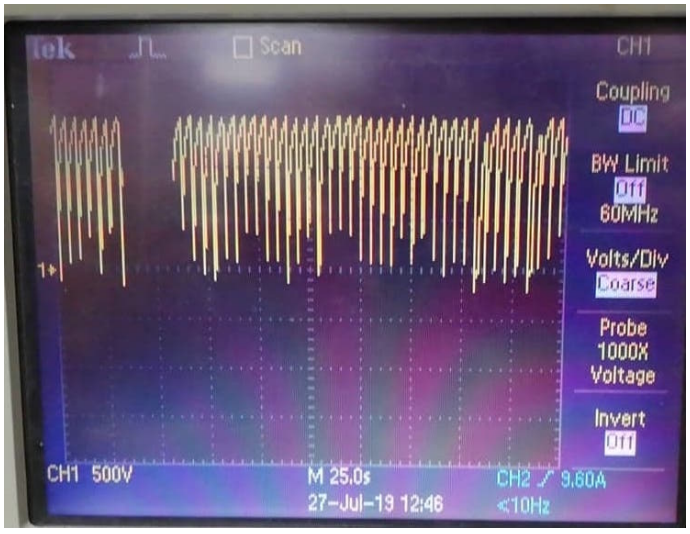

Figure 47: Behavior of the discharge under testing at 0.2 Hz and peak voltage of 1.8 kV. Tektronix TDS2024C

The final set of test lasted for 60 hours bringing a success rate of 92% what means around 40,000 successful discharges. The test was monitored in intervals of 15 hours to ensure the survival of the experiment, and it was ended due a frequent rebooting of the MCU. This was supposed to be because a parasitic fly-back current coming from the coupled inductance. Nonetheless, the circuit performed better even though it presented a huge amount of carbon in the electrodes of the PPT. See Figure 49

As it can be seen in Figure 49b the major layer of carbon is at the tip of the anode of the PPT. This is an interesting effect that has been spotted before [45] with the help of high speed cameras where, once the plasma leaves the electrodes before the capacitor is completely discharged, it will create a *curl back* effect in its attempt to close the circuit even after have been ejected from the discharge chamber. While in 49c can be appreciated how in the area where the SP anode comes out through the cathode of the PPT, presents an erosion and a *whitish* color around it. It is thought to be because now that a higher voltage at the moment of the ignition is reached, the discharge produces a *self-cleaning* effect due the burning of the carbon coating [14].

Another effect that has been mentioned before, is the *rainbow*effect due the erosion of the copper being expelled in the plasma's plume. It is present in all the PPT's case but can be better appreciated in the Figure 49d, where as a extension of the plasma plume it was screened on the vacuum chamber's hatch and on the PTFE base used to support it.

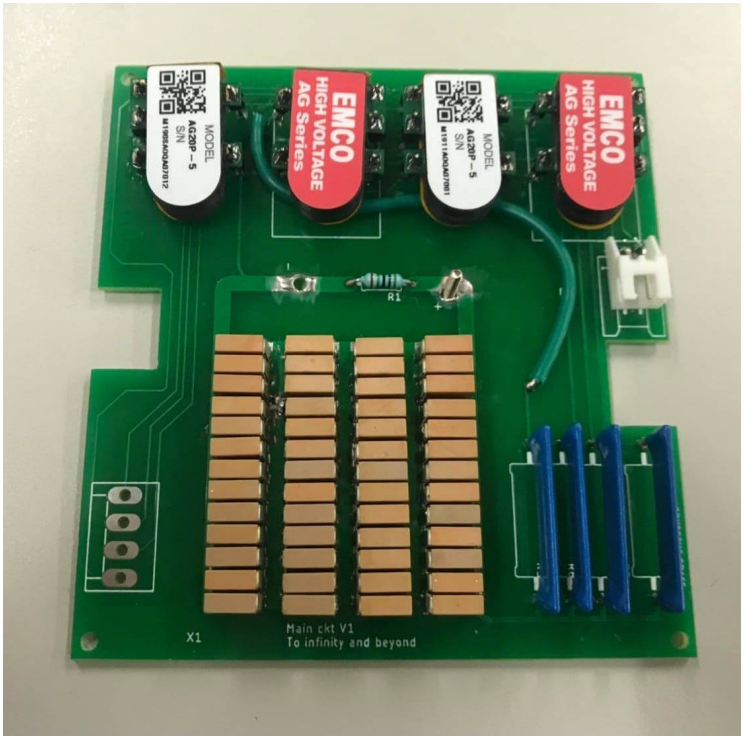

Figure 48: Main discharge circuit PCB

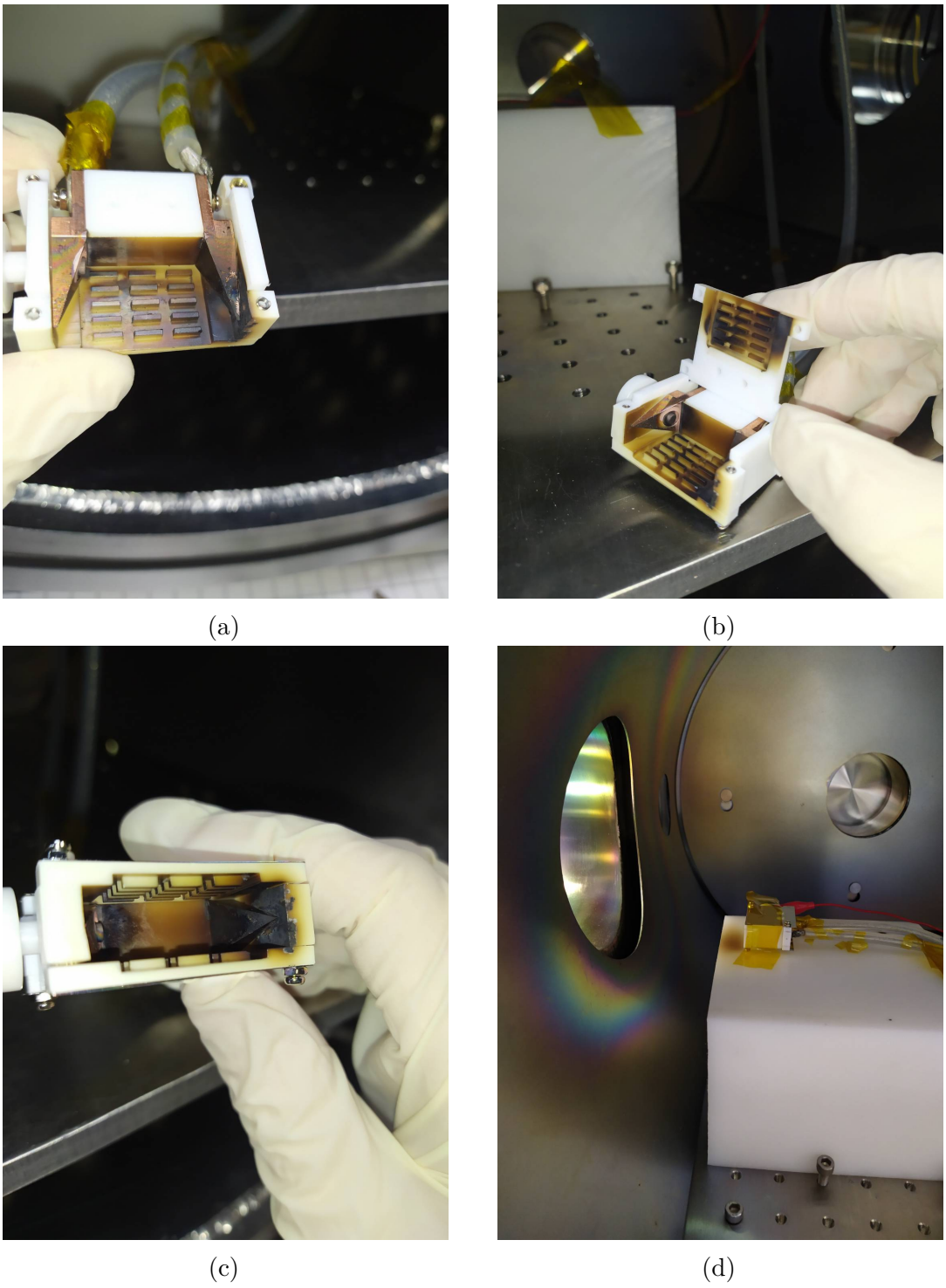

(a) (b)

(c) (d)

Figure 49: 3rd long run test. a) PPT's anode cover by a thick layer of carbon, specially at the tip of it. b) PPT's open case, whitish color around the SP anode. c) PPT's anode, the tip is under a thick carbon layer. d) "Rainbow" effect screened on the chamber's hatch and over the PTFE block.

Intermittently during the test, the current was measured with the help of a

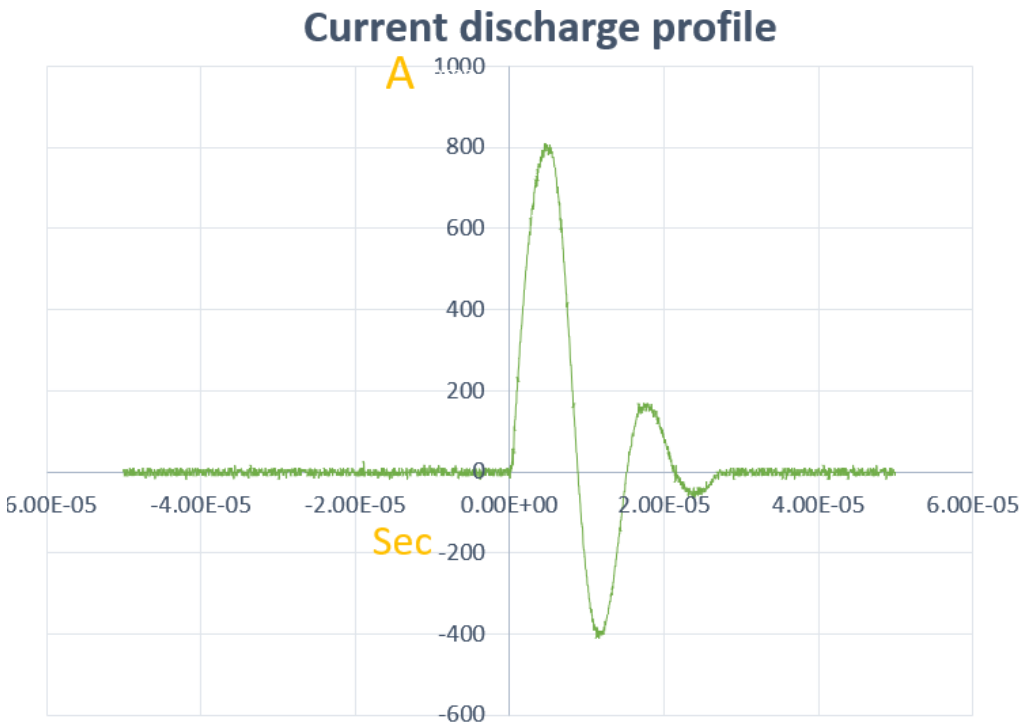

Parameter	Value
Discharge voltage	1750 V
Energy	3.8 J
Impulse bit	6.45 μN

Table 12: Discharge profile and test parameters for I_{bit} measurement.

high current Rogowski coil, which was connected to he Tektronik oscilloscope while measuring the current profile of the main discharge circuit.
This measurements helped to determine the impulse bit of the thruster due its typical extremely low thrust in the order of μNewtons and the lack of a proper test bench for its measurement.

The formula used was the one proposed by Shaw :

$$I_{bit} = \frac{1}{2}\mu_0 \frac{h}{w} \int (I(t))^2 dt, \tag{19}$$

where μ_0 is the permeability of the vacuum, $\frac{h}{w}$ is the aspect radio of the electrodes width/separation gap and the the integral can be approximated to the addition of each sample taken by the oscilloscope. This is possible due its high sampling frequency, giving a theoretical impulse bit of 6.45 μN per discharge. Nevertheless, this is a theoretical approximation because the formula does not take into account the electrodes shape, flare angle, propellant and the ejection of micro-particles that might impact on the total thrust achieved.

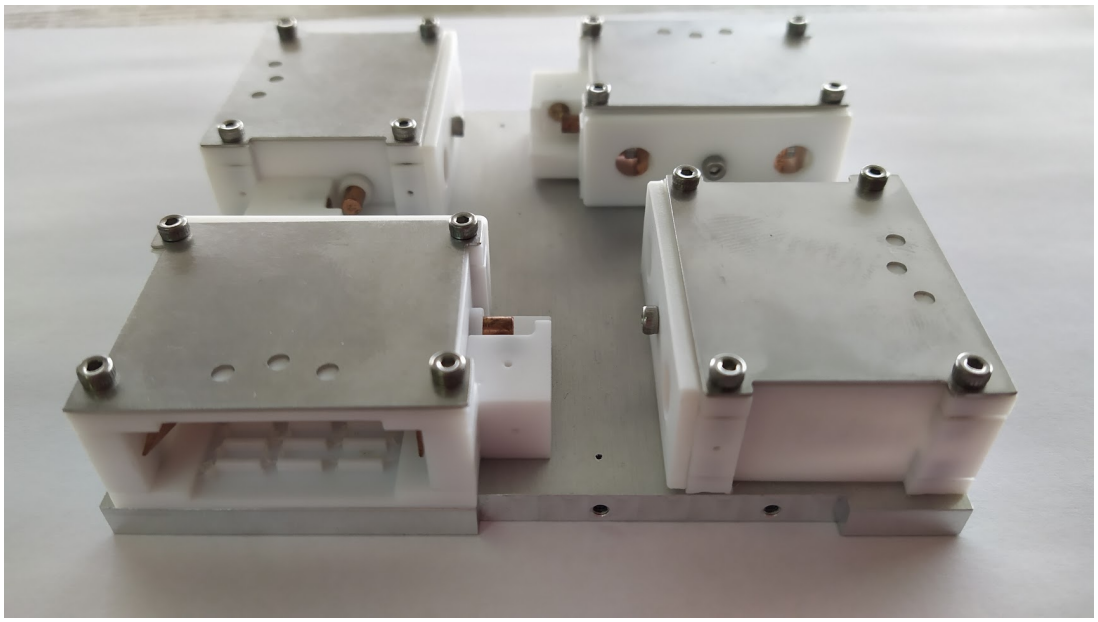

(a)

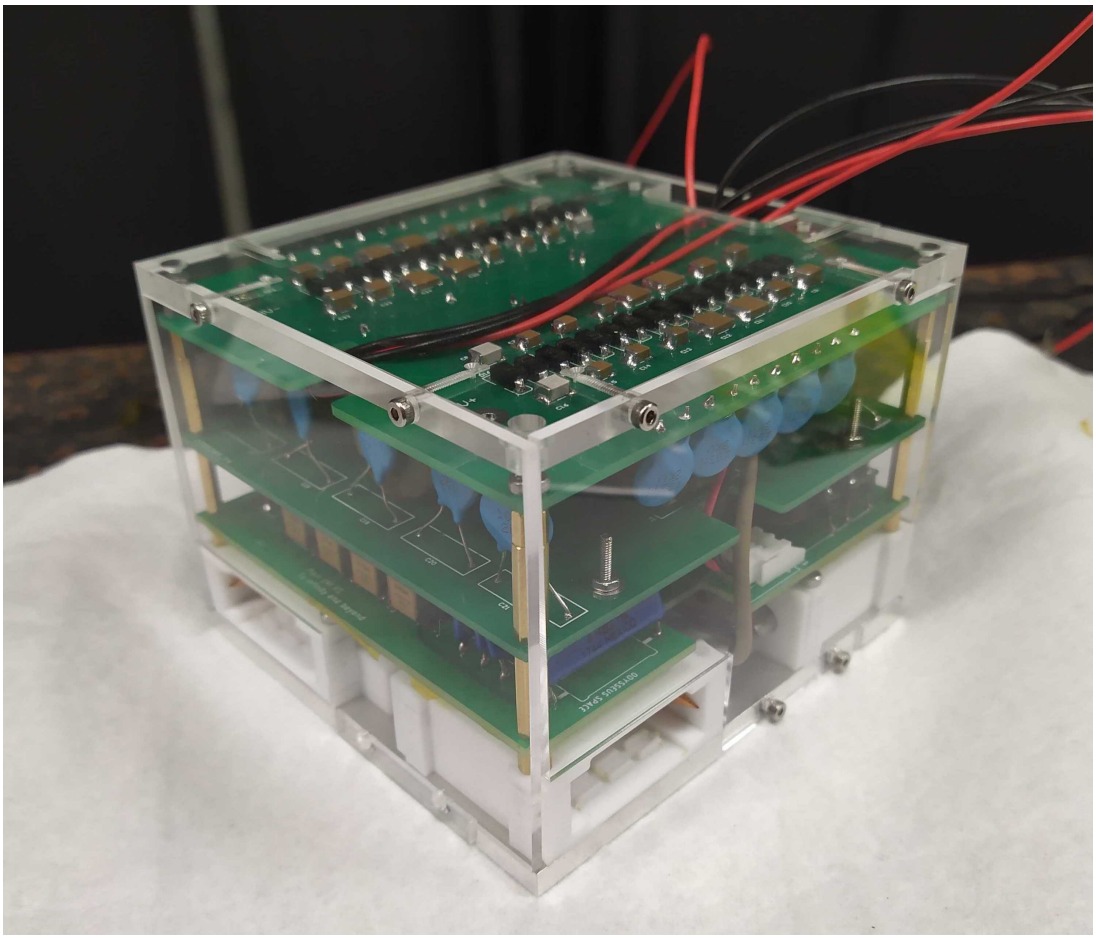

(b)

Figure 50: a) Set of 4 PPTs mounted without electronics, b) Final PPT ACS assembled into 0.8 U.

7 Conclusions

After 5 months of work and have been started from scratch, an engineering model of the ACS PPU was developed. However, as in any *R&D* project, several issues were faced and they must be broken down one by one in order to ensure its future reliable operation once in space.

As it was demonstrated during the realization of this work, the most sensitive subsystem is the ignition circuit or the so called in this thesis *sparkplug circuit*. Where the behaviour of the discharge using the Cockcroft Voltage Multiplier was directly associated with the level of carbonization achieved by the electrodes after a certain number of events. This is hardly predictable, but from the experiments was observed to start causing problems after the first 7,500 discharges although it has been seen by different authors to appear after longer tests. However, other possible reason for this consistent malfunction is attributed to an "overheating" of the insulator in between the set of electrodes, which will influence directly the surface flash-over aimed by the current design.

It is important to clarify that these conjectures are the resulting theories after carried out the experiments and have concordance with the behaviours observed by different authors mentioned during the realization of this work. Moreover, the lack of equipment as an infrared camera and the limited time functioned an important role to determine precisely the causes. Nevertheless, the implementation of different approaches to counter this issues as is the concept brought from the Marx generator, the *spark gap*, tested at the end of chapter 6, could offer an elegant solution to the voltage drop caused by the carbonization on the electrodes and it should be further designed for its application in vacuum and space conditions.

Furthermore, even when the implementation of the flyback with the voltage multiplier was presented and tested over 55,000 successful discharges, it still involves the use of several components and as a result it increase the risk of failure while other topologies as is flyback with extra high gain and circuits without capacitor bank should be deeply investigated.

Finally, the implementation of a better galvanic isolation in between the logic and the power electronics sections to prevent any possible inductive fly-back current that could threat the MCU. As it implies the use of a high frequency inductive driver together with a set of smith triggers for PWM control can be easily implemented to improve the control signal. Moreover, once the control circuit is tested and the prototyping stage is finished, is necessary to change the Atmega328 for a one more suitable for space applications as are the MSP430 and UC3 family of micro controllers from Texas Instrumen or a more reliable MRAM type of memory is recommended.

References

[1] Choueiri, E. Y.,*"A Critical History of Electric Propulsion: The First 50 Years"* (1906-1956),Journal of Propulsion and Power, vol. 20, pp. 193– 203, 2004.

[2] M.Martinez-Sanchez, J.E.Pollard *Spacecraft Electric Propulsion- An Overview* Journal of propulsion and power. Vol. 14, No. 5, Sep–Oct 1998.

[3] Mel'kumov, T. M., (ed.),*Pioneers of Rocket Technology, Selected Works*, Inst. for the History of Natural Science and Technology, Academy of Sciences of the USSR, Moscow, 1964; translated from the 1964 Russian text by NASA as NASA TT F-9285, 1965.

[4] Peter Kindberg *Development of a miniature gridded ion thruster* Master thesis for Erasmus Mundus master program, SpaceMaster. 2017.

[5] Zond 2 NSSDCA catalog. https://nssdc.gsfc.nasa.gov/nmc/spacecraft/display.action?id=1964-078C, November 2019.

[6] Akshay Reddy T.and Atri Dutta *An Overview of Cube-Satellite Propulsion Technologies and Trends* Department of Aerospace, Wichita State University, KS, USA. December 2017.

[7] Sabrina J. Pottinger, David Krejci, Carsten A. Scharlemann *"Pulsed plasma thruster performance for miniaturised electrode configurations and low energy operation"* Surrey Space Center, UK. Acta Astronautica 68, 2011.

[8] Goddard, R.H., *Method, and means for producing electrified jets of gas.*US Patent No. 1,163,037. Application filed October 1917, granted December 1920.

[9] R. L. Burton and P. J. Turchi, *"Pulsed Plasma Thruster"*, Journal of Propulsion and Power, vol. 14, no. 5,1998.

[10] Shaw P.V. *Pulsed Plasma Thruster for small satellites.* Doctoral dissertation, Surrey Space Centre, University of Surrey, 2011.

[11] Qualification of a Micro Pulsed Plasma Thruster (PPTCUP) for Cubesat Application, November 2019: https://www.esa.int/Enabling_Support/Space_Engineering_Technology/Shaping_the_Future/Qualification_of_a_Micro_Pulsed_Plasma_Thruster_PPTCUP_for_Cubesat_Application.

[12] The physics Factbook, an encyclopaedia of scientific essays, December 2019: https://hypertextbook.com/facts/2000/AliceHong.shtml.

[13] F. Guarducci, M. Coletti and S.B. Gabriel *Design and Testing of a Micro Pulsed Plasma Thruster for Cubesat Application* 32nd International Electric Propulsion Conference, Wiesbaden, Germany. September 2011.

[14] Xue-Zhang Fang and Han-Ji Wu *"Spak Plug for Pulsed Plasma Thruster"*, 19th AIAA International Electric Propulsion Conference, Colorado, 1987.

[15] James E. Cooley and Edgar Y. Choueiri *Fundamentals of PPT Discharge Initiation: Undervoltage Breakdown Through Electron Pulse Injection* Princeton University, NJ, USA. 2003.

[16] J. Palencia Electronics for Electric Propulsion, Gridded Ion Technology Airbus Defense and Space Presentation, 26 October, 2017.

[17] Menzel A.B. *Investigation of low-energy PPTs for CubeSats.* Master thesis Luleå Tekniska Universitet and Universite Tolouse-III-Paul-Sabatier, 2018.

[18] S.Ciaralli, M.Coletti, S.B. Gabriel. *Performance and lifetime testing of a pulsed plasma thruster for Cubesat applications.* Acta Astronaut. 47, 291-298, October 2015.

[19] Yunping Zhang, Omar Dary, Adam Patel and Alexey Shasurin. *Investigation of Low Energy Surface Flashover for Initiation of Pulsed Plasma Accelerators* AIAA SciTech Forum, San Diego California, January 2019.

[20] Abdolrahim Rezaeiha, Mehdi Anbarloui and Mohammad Farshchi *"Design, Development and Operation of a Laboratory Pulsed Plasma Thruster for the First Time in West Asia"* Sharif University of Technology, Tehran, Iran, March 2011.

[21] Bingyn Kang and Kay-Soon Low *High Voltage Pulsed Power Supply for the Igniter Circuit of a Pulsed Plasma Thruster* Honolulu, USA,IEEE PEDS, December 2017.

[22] Toshiaki Edamitsu, Hirofumi Asakura, Akinori Matsumoto and, Hirokazu Tahara. *Research and Development of a Pulsed Plasma Thruster in Osaka University* 29th International Electric Propulsion Conference, October31-Novemeber 4, 2005.

[23] Nik Ahmad Kamil Zainal Abidin, Norkharziana Mohd Nayan, Muhammad Mokhzaini Azizan, Azuwa Ali. *Analysis of voltage multiplier circuit simulation for rain energy harvesting using circular piezoelectric* Mechanical Systems and Signal Processing journal volume 101, 211-218, Elsevier. 15 February 2018.

[24] Kavuri Kasi Annapurna Devi, Norashidah Md. Din, Chandan Kumar Chakrabarty *Optimization of the Voltage Doubler Stages in an RF-DC Convertor Module for Energy Harvesting* Universiti Tenega Nasional, Kajang, Malaysia. April 2012

[25] Romei Federico *Pulsed Plasma Thruster Ignition System: Investigation, Test Design and Results* Tesi di Laurea in Sistemi Di Propulsion Avanzati LM, University of Bologne, 2012/2013.

[26] Jason Merritt and Sam Asare. *" Voltage Multipliers and the Cockcroft-Walton generator."* 2009.

[27] I.C. Kobougias and E.C. Tatakis, *"Optimal Design of a Half-Wave Cockroft-Walton Voltage Multiplier with Minimum Total Capacitance."* University of Patras, Greece September 2008.

[28] Nikhil M. Waghamare, Rahul P. Argelwar , *"High Voltage Generation by using Cockcroft-Walton Multiplier."* International Journal of Science, Engineering and Technology Research (IJSETR), Volume 4, Issue 2, February 2015.

[29] Priyen S. Patel and D.B. Dave *"Design, Analysis & Implementation of Negative High Voltage DC Power Supply Using Voltage Multiplier Circuits."* Institute of Technology, Nirma University, Ahmedabad, India, April 2013.

[30] Jie Liu Norbert Henze . *"Reliability consideration of low-power grid-tied inverter for photovoltaic application."* Königstor 59, D-34119, Kassel, Germany, January 2009

[31] Matthew N.O. Sadiku, Sarhan M Musa, Charles K, Alexander *"Applied Circuit Analysis"* McGraw-Hill International Edition. US, 2013.

[32] The Flyback converter. Lecture notes ECEN 4517, Department of Electrical, Computer, and Energy Engineering, University of Colorado. June 2019 http://ecee.colorado.edu/~ecen4517/materials/flyback.pdf

[33] Lisa Dinwoodie. *"Design Review: Isolated 50 Watt Flyback Converter Using the UCC3809 Primary Side Controller and the UC3965 Precision Reference and Error Amplifier."* Texas Instrument Incorporated. 1999.

[34] Riccardo Pittini, Lina Huang, Zhe Zhang and Michael A. E. Andersen. *Primary Parallel Secondary Series Flyback Converter (PPSSFC) with Multiple Transformers for Very High Step-Up Ratio in Capacitive Load Charging Applications.* Department of Electrical Engineering Technical University of Denmark. 2014.

[35] IIT Kharagpur *Fly-Back Type Switched Mode Power Supply* National Programme on Technology Enhanced Learning (NPTEL), Poer Electronics, Lesson 22, Version 2 EE IIT.

[36] Hang-Seok Chol *Design Guidelines for Off-line Flyback Converters Using Fairchild Power Switch (FPS)* Fairchild Semiconductor, Application Note AN4137, 2003.

[37] Jesser James Marulanda Durango, Jhon Jairo Ordonez, Luis Fernando Mosquera Machado *"Design and construction of a Boost type dc / dc converter with adjustable PWM"* Universidad tecnoloogica de Pereira, Colombia. March 2017.

[38] Shiva Moballegh, Sachin Madhusoodhanan, Subhashish Bha acha *Evaluation of High Voltage 15 kV SiC IGBT and 10 kV SiC MOSFET for ZVS and ZCS High Power DC -DC Converters* North Carolina State University Raleigh, NC, USA 2014.

[39] P. A. Laplante and S. J. Ovaska, *"Real-Time Systems Design and Analysis: Tools for the Practitioner"*, 4th Edition. Hoboken, NJ: Wiley, 2012, Chapters 1–3.

[40] Khechiba Kamel and Khiter Anissa. *"Design and implementation of microcontroller based controller for direction and speed of a robot using ARDUINO."* Master thesis, University of Echahid Hamma Lakhdar El Oued, People's Democratic Republic of Algeria, May 2016.

[41] Michael Margolis and Nicholas Welding *"Arduino Cookbook"* O'Reilly editorials First edition, 2011, United States of America.

[42] The Brititsh Museum A history of the world, BBC. May 2019: http://www.bbc.co.uk/ahistoryoftheworld/objects/84v08IiYRb6JSEgOKhcTSw

[43] Glenn Research Center, Pulsed Plasma Trusters, April 2019 : https://www.nasa.gov/centers/glenn/about/fs23grc.html

[44] Glenn Research Center, Propulsion systems, September 2019: https://www.grc.nasa.gov/WWW/K-12/rocket/rocket.html

[45] T.E. Markusic and E.Y. Choueiri *"Visualization of Current Sheet Canting in a Pulsed Plasma Accelerator"* IEPC 1999.

A Appendix

```
///  CODE FOR REED RELAY ATTEMPT  ////
int reed=10;
int pulse=70;
int delay=7000;


void setup() {

    pinMode(reed,OUTPUT);
    pinMode (LED_BUILTIN,OUTPUT);
    digitalWrite(reed,HIGH);
    delay(1000);
    digitalWrite(reed,LOW);
    digitalWrite(LED_BUILTIN,HIGH);
    delay(1000);
    digitalWrite(LED_BUILTIN,LOW);
    delay (1000);

    }
void loop() {
    digitalWrite(reed,HIGH);
    digitalWrite(LED_BUILTIN,HIGH);
    delay(pulse);
    digitalWrite(reed, LOW);
    digitalWrite(LED_BUILTIN,LOW);
    delay(dlay);
}
```

Flyback converter code for PWM control in Arduino UNO and NANO at frequency of 31 kHZ

```
int off=5000;  // Period between pulses
int pulse=200; //pulse length

    void setup() {

    Serial.begin(9600);
    TCCR2B = TCCR2B & B11111000 | B00000001; // for PWM frequency of 31372.55 Hz

    pinMode (LED_BUILTIN,OUTPUT);
    delay(1000);
    digitalWrite(LED_BUILTIN,HIGH);
    delay(1000);
    digitalWrite(LED_BUILTIN,LOW);
    delay (1000);

    pinMode(11,OUTPUT);
    }

void loop() {
if(Serial.available()){}
  analogWrite(11,175);

  digitalWrite(LED_BUILTIN,HIGH);
  delay(pulse);
  analogWrite(11,0);

  digitalWrite(LED_BUILTIN,LOW);
  delay(off);
  }
```

1.PHYSICAL CHARACTERISTICS(mm)

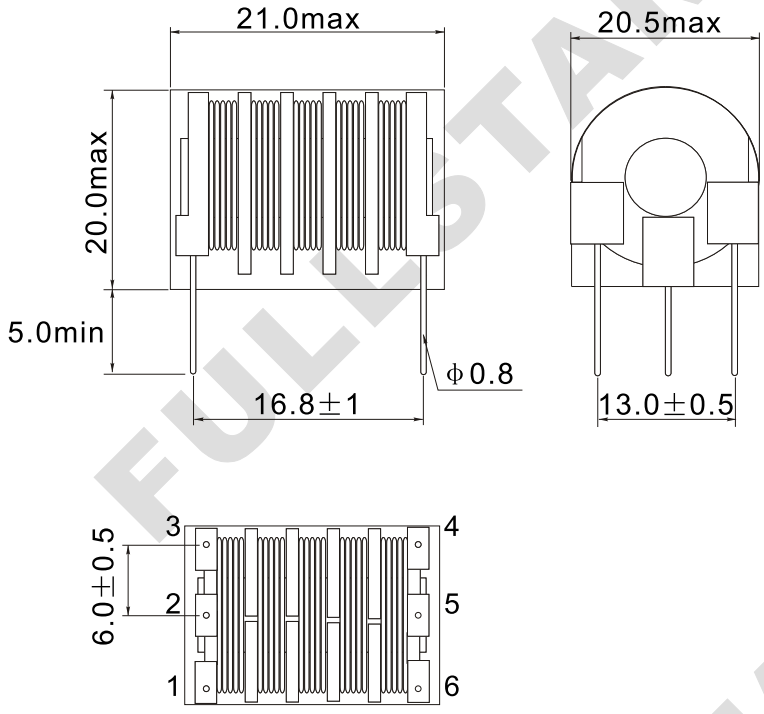

2.ELECTRONICAL SCHEMATIC

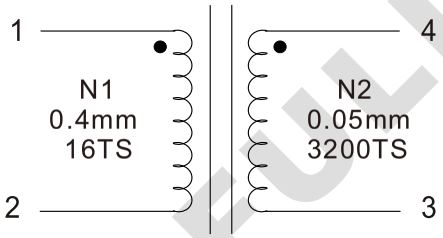

3.ELECTRONICAL SPECIFICATIONS

Turns ratio: 200:1

Inductance(1-2): 55uH

Inductance(4-3): 170mH-180mH

DCR(1-2): 1.4KΩ-1.6KΩ

DCR(4-3): 0.1Ω-0.13Ω

4.MATERIALS LIST

No.	Item	Materials	UL No.	Suppliers
1	Bobbin	5 slot 4 pins		
2	Wire	QA-2 UEW 130℃		
3	Core	R6X15 Mn-Zn		

Note:

1. RoHS Compliant
2. Flammability: UL94V-0
3. ASTM oxygen index: >28%
4. Temp 20℃,48%RH

NAME	High voltage transformers				
CUSTOMER P/N			Date	2019-04-12	
FULLSTAR P/N	FHT0615-201		Rev. A1	Page 1/1	
Drawing changes	Rev.		Drawn. by	Checked. by	Approve. by
	Rev.				